STABILITY ANALYSIS AND MODELLING OF A STRUCTURE WITH CORRUGATED ROOF

NIKOLA TOSOVIC

Master's Dissertation

STABILITY ANALYSIS AND MODELLING OF A STRUCTURE WITH CORRUGATED ROOF

NIKOLA TOSOVIC

Abstract

Corrugated galvanized iron (CGI), or corrugated sheet metal, is a lightweight roofing material that was invented in the early 1800s. The corrugation gives the steel an increased flexural strength in its installed direction and thus increases the amount of load the CGI-plate is able to carry and the span it can be effective at. Thanks to its light weight, corrugated sheet is one of the most commonly used roofing materials for warehouses and other large premises in Sweden as of today.

When the CGI-plate is installed as the roof, it is typically screwed to the top-chord of a roof truss. When installed, the sheeting is stiff, but its in-plane stiffness decreases when deformation occurs, due to second-order effects. Since it is connected to the top chord, its in-plane stiffness is also dependent of the top-chords deformation. Consequently, this will affect its stabilizing capabilities in a negative way and the rigidity may not be sufficient to prevent buckling of the trusses' compressed parts. To counteract this phenomenon, it is usually recommended to either use a thicker profile for the CGI-sheets or to use some type of horizontal bracing in the plane of the roof.

To examine how the buckling of the top chord would affect a structure like this, a model of a part of a typical warehouse was designed in the program ROBOT to decide the dimensions of the structural components. The model included three roof truss beams on supports, and the CGI-roof placed on top of the truss beams. When all building elements were designed, the same part of the warehouse was modelled in the program Abaqus. Apart from analyzing the buckling behavior, another important objective was to gain more knowledge about how a roof of this type should be modelled in Abaqus and how much the CGI-thickness and the flexibility of the connectors used to fasten the roof would affect the results.

The simulation made in Abaqus consisted of: first order (small displacement) linear analysis, large displacement non-linear analysis, linear buckling analysis and a non-linear buckling analysis. The linear buckling analysis showed that, for the most relevant load cases, it is in fact not the top-chord of the truss that will buckle, but instead the bottom-chord of the middle-truss. The buckling load found represents a load of approximately 5,5 times a design load case.

Three different models of the roof were tested, one where the roof was modelled with a large number of CGI-plates, one with only two large CGI plates and one with only one big CGI plate. The aim was to examine if there was any difference in the result between the different modelling approaches. The different analyses showed that the configuration of the CGI-sheets did not have any major impact on the result.

The buckling load and the deformation pattern of the structure changes with the connector stiffness since the load distribution changes with it. With rigid connections the applied distributed load on the roof was distributed to the three main trusses as 20/60/20%. More flexible connectors changed the distribution to 25/50/25% instead, with marked changes of the deformation pattern. The buckling load also changes with the connector stiffness, since lesser load is distributed to the middle truss with more flexible connectors. The more flexible connectors allow the elements to move which makes them a bit more flexible which also increases the buckling load.

When the sheeting thickness was increased the result showed that the load distribution was changed to resemble a 33/33/33% distribution. This changed the deformation of the structure,

but it could be concluded that the deformation decreases everywhere except on the outer top-chord, because of the change in load distribution. The buckling load increased with thicker CGI-sheets. With a four times thicker CGI-plates the buckling load increased with 8,5%, which is not much considering the cost for the extra material.

The results from the thesis are based on ideal conditions and should be considered as indicator for how it would behave in the real world with imperfections, horizontal loads, different spans and profiles. However, it is concluded that the bottom-chord rather than the top chord is of concern as regards the risk of buckling and should be braced when designing structures of this kind.

Sammanfattning

Korrugerad plåt (TRP-Plåt) är ett lätt takmaterial som uppfanns i början av 1800-talet. Korrugeringen ger plåtskivan en ökad böjhållfasthet i dess installerade riktning. Eftersom dess böjhållfasthet ökar, ökar även den last som TRP-plåten kan bära och den spännvidd som den kan vara effektiv på. Tack vare sin lätthet är korrugerad plåt ett av de mest använda takmaterialen för lagerbyggnader och andra byggnader med stora spännvidder i Sverige.

När TRP-plattan är installerad som tak, skruvas den fast på överflänsen på den fackverksbalk som utgör takets bärverk. Takplåten har hög styvhet i planet, men dess styvhet minskar när deformation uppstår på taket, på grund av andra ordningens effekter. Eftersom takplåten är ansluten till fackverksbalken, är dess styvhet i planet också beroende av fackverksbalkens deformation. Följaktligen kommer detta också att påverka dess stabiliseringsförmåga på ett negativt sätt, och dess styvhet kanske då inte är tillräcklig för att förhindra knäckning/buckling av tryckta delar. För att motverka detta fenomen rekommenderas det vanligtvis att antingen använda en tjockare profil på TRP-plåten eller att använda någon typ av horisontell stabilisering i takets plan.

För att undersöka hur den fackverksbalkens knäckning påverkar en struktur av denna typ, designades en del av ett typiskt lager i programmet ROBOT för att bestämma byggnadselementens dimensioner. Modellen bestod av tre fackverksbalkar på stöd, och TRP-plåt som tak ovanpå fackverksbalkarna. När alla element var designade, modellerades samma byggnad i programmet Abaqus, där olika analyser utfördes. Förutom att undersöka stabilitetsfenomen, var ett annat viktigt mål att få mer kunskap om hur ett tak av denna typ skall modelleras i Abaqus och hur mycket TRP-tjockleken och eftergivligheten i förbindarna mellan takelementen påverkar resultaten.

Simuleringarna gjorda i Abaqus bestod av: linjärelastisk analys (små deformationer), icke-linjär analys (stora deformationer), linjär bucklingsanalys och en icke linjär bucklingsanalys. Bucklingsanalysen visade att det i själva verket inte var den övre delen av fackverksbalken som var i riskzonen för knäckning, utan det var i den undre delen av fackverksbalken där knäckning uppstod. Egenvärde visade sig vara 5,5, dvs en 5,5 gånger större än den pålagda lasten i analysen, som svarade mot en ungefärlig dimensionerande last, skulle motsvara knäckning.

Tre olika takmodeller testades, en modell bestod av många TRP-plattor, en med bara två stora TRP-plattor och en med bara en stor TRP-platta. Detta gjordes för att undersöka om det var någon skillnad i resultatet mellan dem. De olika analyserna visade att konfigurationen av taket inte hade någon större inverkan på resultatet.

Egenvärdet och strukturens deformation ändras när förbindarnas styvhet ändras, eftersom lastfördelningen mellan takbalkarna påverkas. Med styva förbindare fördelades den pålagda lasten på taket med 20/60/20% på de tre fackverksbalkarna, vekare förbindare ändrar fördelningen till 25/50/25%, vilket förändrar deformationen i strukturen. Egenvärdet förändras också eftersom en mindre andel av den pålagda lasten tas av den mittersta fackverksbalken. De eftergivliga fördbindarna gör det också möjligt för elementen att röra sig mer, vilket ökar egenvärdet.

När plåttjockleken ökades visade resultatet att lastfördelningen även här ändrades, med fördelningen 33/33/33%. Detta förändrade deformationen i strukturen. Det kunde konstateras att deformationen minskade överallt utom på de yttre fackverksbalkarna, detta på grund av den ändrade lastfördelningen. Egenvärdet ökade med tjockare TRP-plåt. Med fyra gånger tjockare TRP-plattor ökade egenvärdet med 8,5%, vilket inte är mycket med tanke på kostnaden för det extra materialet.

Resultaten är baserade på idealiserade förhållanden och bör betraktas som en fingervisning för hur det skulle kunna se ut i verkligheten. I verkligheten förekommer imperfektioner, horisontella laster, andra spännvidder samt olika profiler, vilket påverkar resultaten. Den slutliga bedömningen är att fackverksbalkens underfläns snarare än dess överfläns bör stabiliseras med horisontella stöd vid utformning av fackverk/TRP strukturer för att försäkra att strukturen är tillräckligt stabil och kan bära lasten under hela sin livslängd.

Preface

This master thesis covers 30 credits and was carried out as a joint project at the Division of Structural Mechanics at the Faculty of Engineering, Lund University and Ramboll in Malmö.

I would like to thank my supervisor, and the one who came up with the subject of the thesis, Arash Roohbakhsh for all the input and guidance I received during the work. I would also like to thank Ramboll who offered a workplace at their office in Malmö during the whole semester.

Also, a big thank you to my supervisor at the Division of Structural Mechanics, Erik Serrano, who helped me transform the idea to an actual thesis, for always having his door open for questions and his willingness to help.

Lund, February 2020

Nikola Tosovic

Table of content

1. Introduction

1.1 Background

The corrugated sheet is one of the most commonly used roofing materials for warehouses and other large premises in Sweden as of today. Corrugated galvanized iron (CGI) is a lightweight roofing material that was invented in the early 1800s. The corrugation of the steel sheets gives the lightweight material an increased strength and stiffness (Shelter cluster)(Hanses, 2015). The corrugation increases the flexural strength in direction X as seen in fig.1.
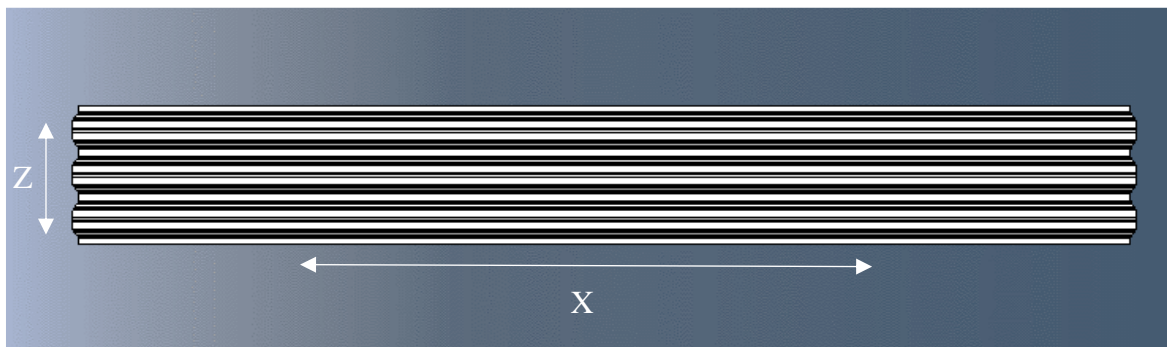
Figure 1. The directions of the CGI-plate. The coordinates refer to the global coordinates of fig.2.

When installed onto the roof, they sheets are installed in direction X. The idea is that the roof sheet, through the rigidity of the sheet plate, should prevent buckling of the upper chord of the roof truss when it is subjected to axial compressive forces due to the bending of the truss. The corrugated sheets are used thanks to their ability to carry load over large spans, but also because of their ability to carry heavy loads in relation to their weight and material costs. A typical hall structure with CGI-plates as roof is shown in fig.2.
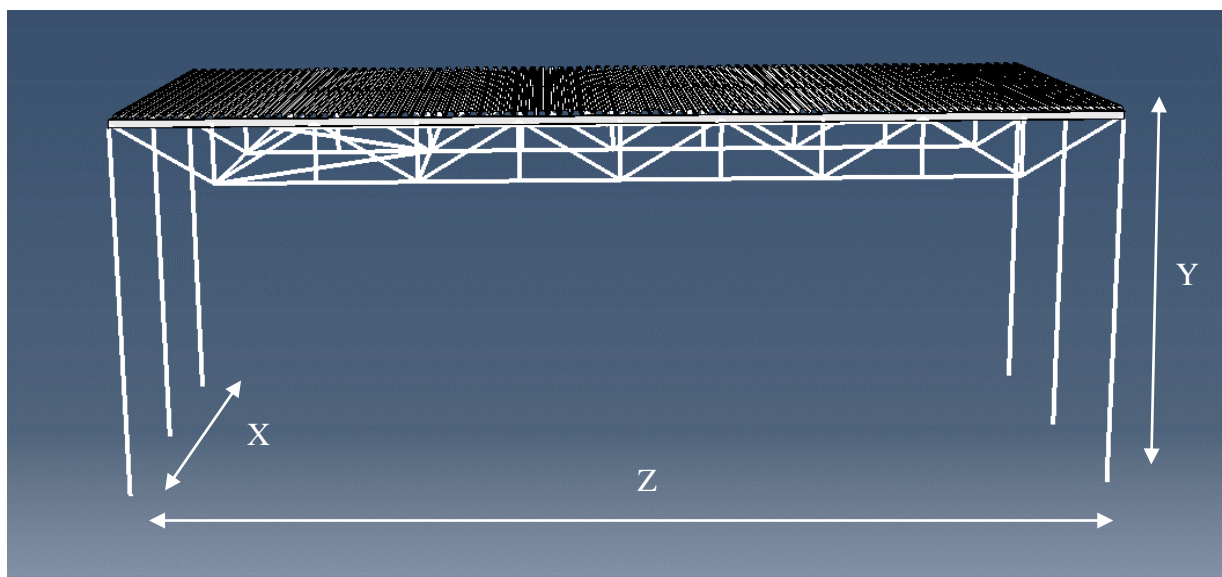
Figure 2. The global coordinates used for the thesis.

When the sheet plate is deformed due to vertical loads (e.g. snow load) the stiffness of the sheet plates will decrease, due to second-order effects. Consequently, this will also affect its stabilizing capabilities in a negative way and the rigidity may not be sufficient to prevent buckling of the trusses' compressed parts.

Since the sheet plates are connected to the trusses' top chord, the deformation of the truss parts will also affect the sheet plates' deformation and the overall stability of the structure.

Two ways, that are commonly used, to counteract this from happening is to either increase the thickness of the CGI-plates or to use some type of additional horizontal support, usually bracing, on the truss so it is able withstand the deformation that occurs and provide the stiffness needed. While the increased thickness will make the roof stronger and stiffer, it will also increase material usage.

In today's typical designs, the roof sheets are usually made thicker to account for these phenomena.

1.2 Aim and objective

The aim is to gain knowledge of how CGI-plates should be modelled in Abaqus and to examine how the CGI-plates affect the overall stability of the structure.

The objective is to study an extracted part from a warehouse (for dimensions and profiles see chapter *1.5 Warehouse*) that will be designed in the program ROBOT and then modelled in Abaqus.

Research questions

A.   What part of the structure is most prone to buckle?

B.   Is it possible to continue the modeling of CGI the way that it is done today?

C.   How should the computer modeling of CGI-plates be done in projects like this?

D.   How does the increase of CGI-thickness affect the structure with respect to buckling?

The overall purpose of this work is to contribute to increased knowledge about how this type of structures can/should be modelled and to increase the knowledge of the structural design of CGI-plates.

1.3 Method

The analysis will be done in two parts. The first part of the analysis will include the design of a warehouse. This is done through the software ROBOT, where a model of a warehouse will be designed. ROBOT is a structural analysis software used for design. Different linear and non-linear analyses are possible to perform in this software. A simple analysis will be made to ensure that the building can withstand the loads it would be exposed to in reality.

This model will later be remodeled in the second software, Abaqus, which is a software suited for finite element analysis and computer-aided engineering. The analyses made in Abaqus will consist of linear, non-linear and buckling simulations. The objective is to start with a complex model and then to simplify the model as much as possible without affecting the results.

A parametric study will be made to examine how the modelling of the sheeting, including the sheeting thickness and connector stiffness will affect the results in terms of buckling behavior.

1.4 Limitations

- Plasticity will not be taken into account.
- Only one type of building will be studied which means that the width and length of the building is fixed.
- Only one load type is examined (vertical load, uniformly distributed)
- The material will only consist of steel S355.
- Imperfections will not be included.

1.5 The warehouse

The warehouse model used throughout the thesis is modelled to resemble extract from an ordinary warehouse in Sweden. The geographic location of the warehouse is in Malmö, Sweden.

The geometry of the warehouse was provided by Arash Roohbakhsh, senior consultant at Ramboll, as it reflected a typical Swedish warehouse. The geometry that was the basis for the warehouse can be seen in fig.3, 4 and 5.
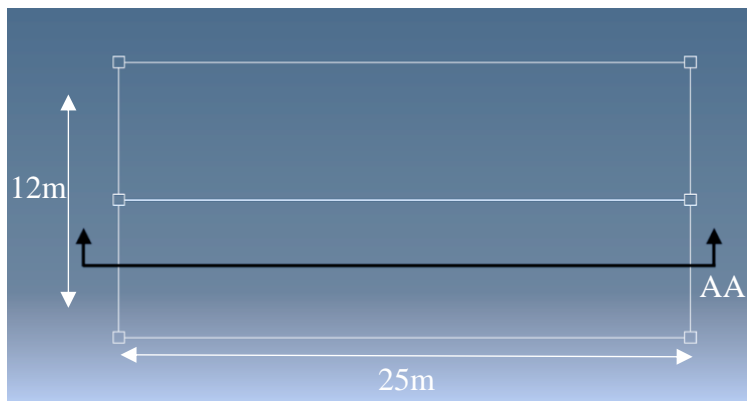
Figure 3. An overhead view of the warehouse.

3
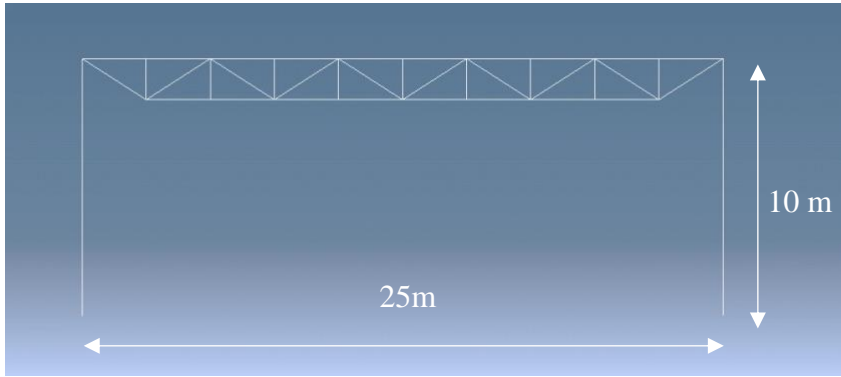
Figure 4. Section AA of fig.3, showing the truss and columns.
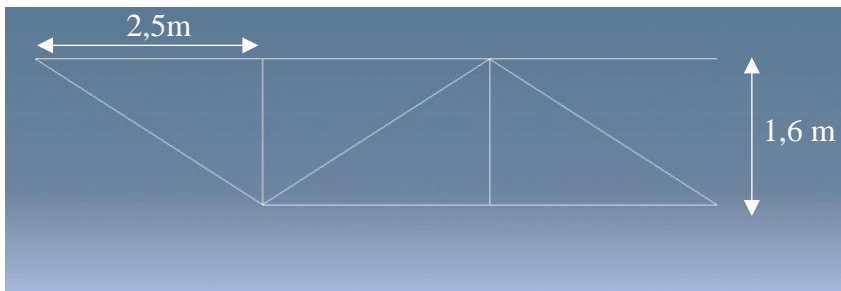
Figure 5. A detailed view of the truss.

This warehouse was later modeled in ROBOT and two loads, a dead load $(1kN/m^2)$ and a snow load $(1.5kN/m^2)$, was then added on top of the building. Through a non-linear simulation using these loads, the result indicated that the building elements were of correct dimensions to withstand the deformation. The used structure can be seen in fig.6. and an overall look over the profiles, dimensions and length used for all the elements can be seen in table 1.
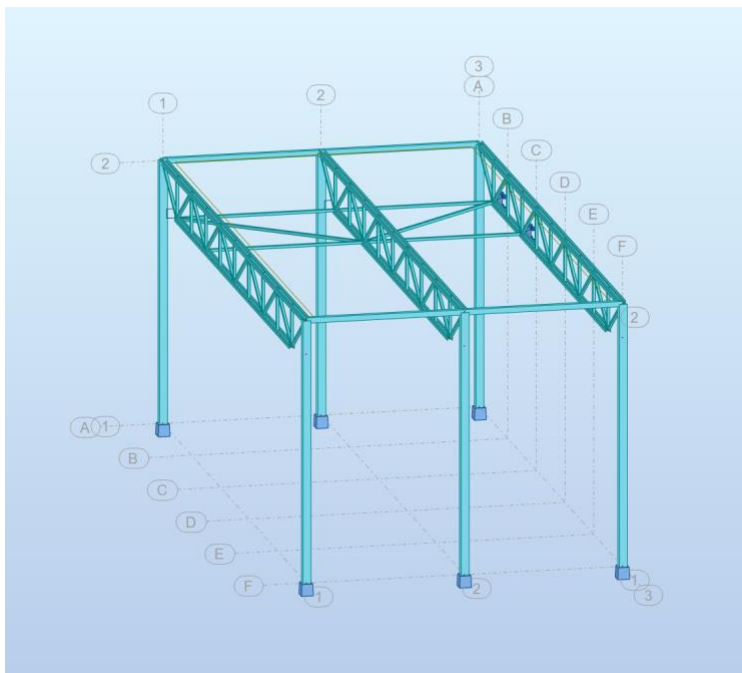
Figure 6. The structure visualized in the program ROBOT.

4

Table 1. Overview of elements used when modeling the structure in ROBOT.

Element	Profile	Dimension(mm)	Length(m)
Colum	HEB	300	10
Top-Chord	HEB	220	25
Bottom-Chord	HEA	200	20
End-Beam	HEA	200	6
Web-Vertical	VKR	100×100×5	1,6
Web-Diagonal	VKR	100×100×5	2,97
Bracing-Horizontal	VKR	100×100×5	6
Bracing-Diagonal	VKR	100×100×5	7,81

2 Governing theory

2.1 Steel

Steel as a building material has grown in importance ever since humanity has been able to make steel. It was shown to be a groundbreaking building material as early as 1889 at the world fair in Paris. Steel structures with large spans that were easy to dismantle were already possible and known to work due to the construction of the Crystal Palace in the year 1851. The destruction of the Crystal palace by fire, 1936, also showed the dangers of using steel as a building material (Hanses, 2015).

Since then a lot has happened. Steel construction methods have been developed based on the specific qualities of the material, and steel has revolutionized both architecture and construction. Its many uses have made steel one of the most versatile building materials, from high-rise buildings and transparent building envelopes to large halls filigree construction. It can be used as reinforcement in concrete and facade cladding as well as lightweight material. With its versatility, it is no surprise why steel is one of the most common building materials in the world today (Hanses, 2015).

2.1.1 Material Properties

Steel's compressive and tensile strength are almost equally high. This makes steel suitable for usage alone, without the combination of another material. One of the weaknesses steel has is its sensitivity to corrosion and that it does not have a natural protection against thermal loads, which makes fire protection for steel a high priority. It is important to make sure that adequate covers and protection are used when steel is combined with another material (Hanses, 2015).

Steel is a type of metal, but the mixture of iron and carbon along with other materials also makes steel an alloy. Metals are usually divided into ferrous and non-ferrous metals. Steel has a carbon content of less than 2%, which makes steel a non-ferrous metal. The characteristics of a metal is usually that it has a high density and strength, a high melting point and good conductivity for heat and electricity. Steel has very well embraced these characteristics (Hanses, 2015).

2.1.2 Structural steel

The introduction of the European standards changed the designation system of steel. The two most important steel types for construction are called S235 and S355. S235 and S355 are a type of fine-grained steel. Fine-grained steel has high strength and toughness compared to other types of steel. It achieves these qualities through the reduction of the grain size. The smaller grain size is achieved by using particular elements as alloys, a low carbon content (<0.20%), and with a special heating and rolling technology. Its low weight and combined with high strength makes this type of steel suitable for bridge-building. The higher strength and toughness also makes it suitable for welded connections (Hanses, 2015).

2.1.3 Shaping

When metals are subjected to high stress, plastic deformation takes place. Therefore, in using steel it is not necessarily the failure load that is decisive but the stress at which an excessive deformation is reached. This limit is called the yield limit and is sometimes defined as the level

resulting in 0.2% of irreversible (plastic, permanent) strain. A stress/strain diagram (fig.7) is usually drawn to assess the elasticity, plasticity and strength in the steel (Hanses, 2015).
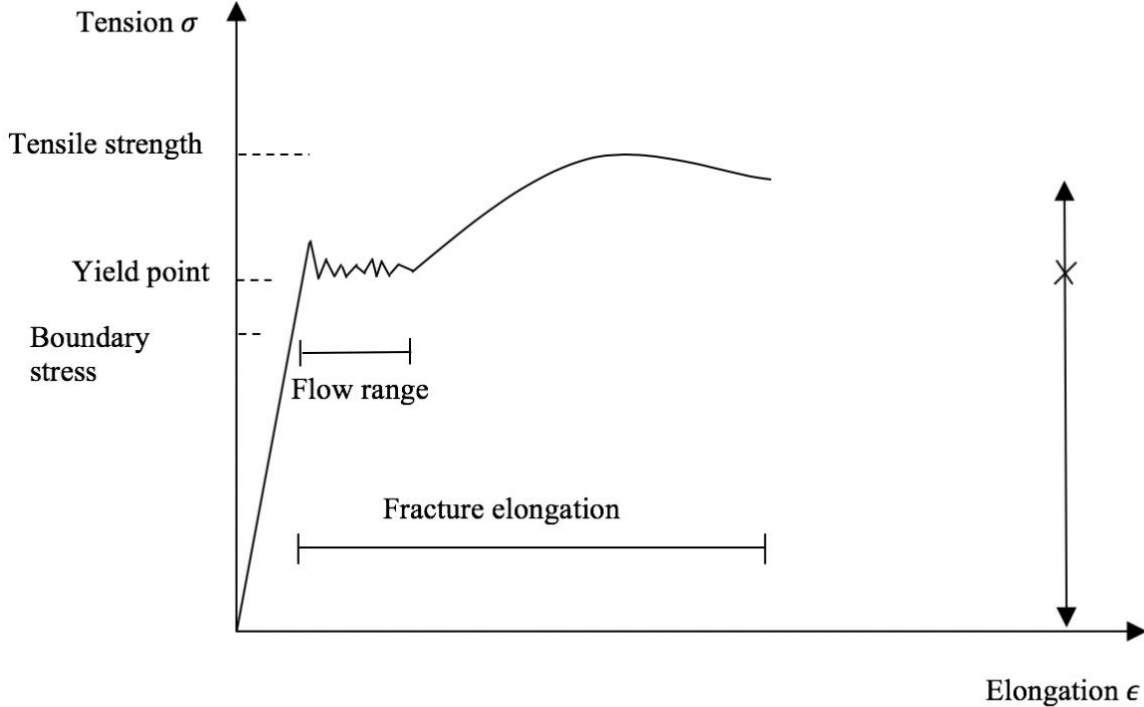
Figure 7. A typical stress/strain diagram for steel. Adapted from (Hanses, 2015).

2.2 Corrugated galvanized Roof sheets

2.2.1 History

Corrugated roofing was invented 1820 by a man named Henry Palmer. Henry Palmer worked for the London Dock Company and came up with the idea when assisting with the building of a new warehouse near the docks. Since the warehouse was big and the roof would weigh a lot, Henry came up with the idea of the lightweight corrugated roofing sheets. He sold the patent for the lightweight roof rather quickly to a carpenter (World Archaeolgy, 2008).

In the 1840s the corrugated roof was starting to be used more on new buildings such as the Eastern Counties Railway Station and the Nine Elms gasworks, both located in London. The corrugated roof sheeting was positive in many ways, such as their ability to be taken down, transported and the put up again rather quickly. The quick reassemble/disassemble of the corrugated roof came in handy when the roof started to corrode. By hot-dipping the sheets in galvanization, this problem was largely solved. Corrugated roof was soon popularized and synonymous with railway stations. In 1843, the patent for corrugated roof ran out and competition started to saturate the market (World Archaeolgy, 2008).

Even though the corrugated roof was an engineering feature it was not aesthetically pleasing, but because of its lower price it was able to take over the market. During the goldrush in California in the 1850s, a lot of housing had to be available because of the quick increase of population in the area. For the most part, the houses were either tents or prefabricated wooden huts, but a company from New York saw an opportunity and send 500 huts made of iron with corrugated roof to California. These iron huts where cheaper, fireproof and more comfortable which made them grew in popularity. Soon after, even the British companies saw the opportunity and started sending iron buildings to California.

It was not only in California that opportunities raised. The Liverpool based manufacturer "Francis Morton and Co" concentrated on the mining communities in South and Central America and started to supply these communities with working barracks and hospitals.

When the gold rush started in Australia, all these companies where eager to send barracks and housing there. This way iron buildings and, mainly, corrugated roof, was spread over the world (World Archaeolgy, 2008).

2.2.2 Structure

There are different types of profiles for different sheets, but their structures are the same. A typical profile can be seen in fig.8.
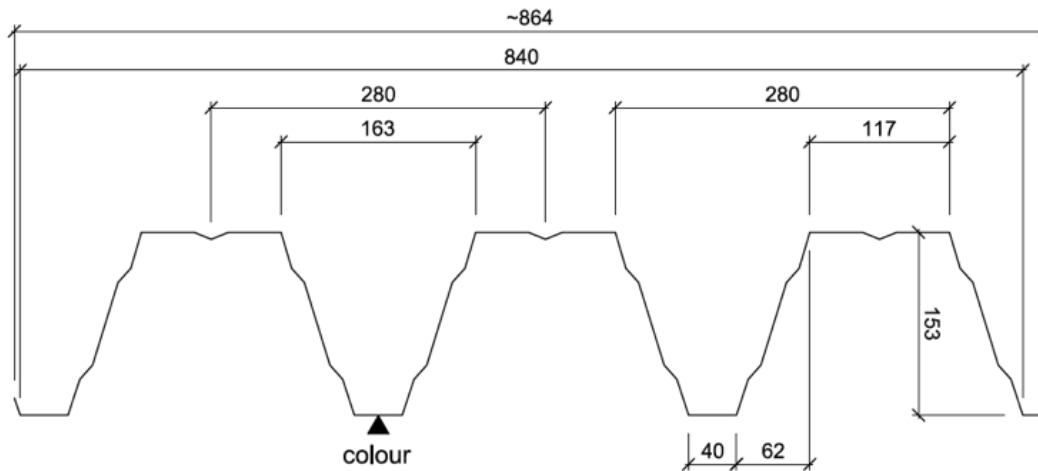
Figure 8. A typical profile used for CGI plates. Note that the distances changes between different profiles. From appendix A, Rukki technical drawing.

Depending on the design load and span, the height and the width of the sheet, can either increase or decrease.

The corrugation of the metal sheets increases the bending stiffness in all its directions compared to a non-corrugated sheet. Thanks to the stiffness increase a larger load and a larger span is possible to use.

2.2 The finite element method

The finite element method is a numerical method used to solve differential equations that are difficult, or even impossible to solve using an analytical method. The differential equations can be solved in an approximate manner with a numerical method, making it possible to take into account complex geometries and boundary conditions which in many cases would be impossible using analytical approaches (Petersson & Ottosen, 1992).

The differential equation/equations that are used to describe the problem are assumed to hold over a certain region. The region may be one, two or three-dimensional. This region is then divided into smaller parts, so called finite elements, and the approximation is then carried over each element. Even though there are variations in the variables over the whole region, it is typically assumed that the variables have a limited variation (e.g. a linear) within an element. A group of small elements over a region is called a finite element mesh. The mesh can look different depending on the region geometry and the accuracy of the model is directly connected to the mesh. A finer mesh will give a more accurate result then a coarse mesh would (Petersson & Ottosen, 1992).

Different types of approximations can be used for each of the elements. Depending on used approximation type different corresponding behaviors can be determined. This is made possible because of the simplicity of the approximation over every element. The elements are then patched together which makes it possible to obtain approximate solution for the entire body (Petersson & Ottosen, 1992).

10

There are five things that determine the character of the FE-mesh; element family, degrees of freedom, number of nodes, formulation and integration.

2.2.1 Family

There are different types of elements to choose between when modeling a structure in a FEM software. Depending of what element type is used, different things are possible to model. One should always weigh each modeling decision between accuracy and calculation time. The problem that should be modeled determines the element type. Commonly used elements include solid elements, shell elements and beam elements, see fig.9 (Sharcnet, u.d.).
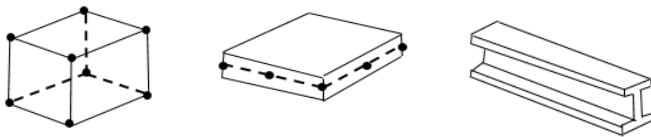
Figure 9. Different element types adapted from (Sharcnet, u.d.).

2.2.1.1 Solid elements

A solid element can refer to a two-dimensional or three-dimensional model. The two-dimensional solid element allows for plane and asymmetric problems while the three-dimensional element allows for a more complex modelling including several layers of different materials in different orientations. (Sharcnet, u.d.)

The solid element library in Abaqus includes isoparametric elements: quadrilaterals in two dimensions and "bricks" (hexahedra) in three dimensions. These isoperimetric elements are usually preferred in most cases because of their cost-efficiency (Sharcnet, u.d.).

Solid elements should be used sparsely. It is the most calculation heavy element of the three element types, but it can also give a more accurate result. Depending on what you want to examine in the model, a solid element can be preferred (Sharcnet, u.d.).

2.2.1.2 Shell elements

Abaqus offers shell elements that allow the modelling of curved, intersecting shells that can exhibit nonlinear material response and undergo large overall motions (translations and rotations). There are three different categories of shell elements to choose between; general-purpose, thin and thick shell elements. One should choose category depending on what the problem is. If the problem can be sufficiently described as a classical (Kirchoff) shell theory, then a thin shell should be used. Thick shells should be used as a solution for problems best modelled by shear flexibility. The general-purpose shell element can provide solutions for both thick and thin shell problems (Sharcnet, u.d.).

Shell elements are more cost-effective than the solid element but more cost heavy than the beam element. Its thickness is assigned, and taken into account in the calculations, but the element geometry is two-dimensional.

2.2.1.3 Beam/line element

The beam/line element is the least complex element of the three. It is also the element that is most cost-effective because of its simplicity. Sections can be assigned to the line element to resemble different beams such as I, H and box cross sections (Sharcnet, u.d.).

A beam element, in the context of Abaqus, is an element that works under the assumption that the problem is reduced to one dimension and that the primary solution variables are functions of position along the beam axis only (Sharcnet, u.d.).

2.2.2 Degrees of freedom

A degree of freedom represents a basic variable in the model, and for structural problems it determines in what way/ways a model can move and deform. The degree of freedom is one of the most important factors for the result in a simulation. All other outputs are based on the degree of freedom the model has been assigned. In a stress/displacement simulation the degree of freedom is usually for the translations at each node, while some element families, such as beam and shell element, also have rotational degrees of freedom (Sharcnet, u.d.).

2.2.3 Number of nodes

The degree of freedom is defined at every node, which means that the solution of the primary variable is obtained at the nodes. This also means that there is no direct information that the software can use between the nodes. To still be able to calculate and show what is happening between the nodes, the software uses an interpolation between the nodes (Sharcnet, u.d.).

There are different element types one can choose from depending of the model. The composition and difference for three different element types can be seen in fig.10.
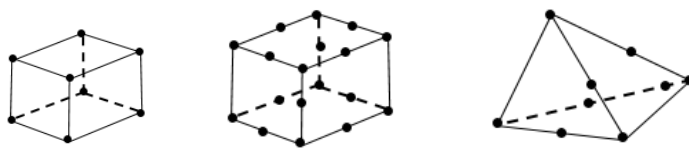
Figure 10. Composition of different types of nodal elements adapted from (Sharcnet, u.d.).

The interpolation in the three different elements are different. The interpolation in a linear brick element is, as the name implies, linear between the nodes while the quadratic brick uses a quadratic interpolation. The linear brick is composed of eight nodes while the quadratic brick is composed by twenty nodes. The tetrahedral is made of ten nodes and uses a modified second order interpolation (Sharcnet, u.d.).

While the distances between nodes are closer and the greater number of nodes contribute to a more accurate result, it also costs a lot of computer power. Linear bricks are usually enough, depending on the model and interactions. One should avoid using tetrahedral elements as much as possible. It is less accurate than the other options on simple models. Tetrahedral elements

can be favorable on complex models, such as models with complex and curved shapes, for example (Sharcnet, u.d.).

2.2.4 Formulation
The formulation describes what mathematical theory is used to define the elements' behavior. Different formulations can be used depending of the problem. The Lagragian formulation is usually used for stress/displacement problems. The formulation alludes that a material that is associated with an element, will be associated with that same element through the whole simulation. This means that the material cannot flow between element boundaries (Sharcnet, u.d.).

2.2.5 Integration
The integration is used to calculate the stiffness matrix. There are different techniques for this integration. Abaqus uses Gaussian quadrature for most elements. Some elements can use full integration or reduced integration. The difference between a full integration and a reduced integration is that the full integration is more accurate than the reduced integration, but it is also more computer costly. The choice between a full integration and a reduced integration is case dependent, but a reduced integration can in most cases be used without any major impact on the result, although non-physical deformation patterns known as spurious zero energy modes can occur (Sharcnet, u.d.). In some cases, a reduced integration can in fact improve the accuracy of the otherwise overly stiff FE-model.

2.2.3 Nonlinearity
There are different types of nonlinearities such as geometrical nonlinearity, which includes finite deformations; physical nonlinearity, which includes material nonlinearity and stability problems; nonlinear boundary conditions and coupled problems (Wriggers, 2008).

This thesis will focus on geometrical nonlinearity.

2.2.3.1 Geometrical nonlinearity
Since many parts of a structure can only be affected by small strains before its usability begins to decline, it is usually enough to consider small deformations and strains in structural mechanics. A linear constitutive equation can be introduced when elastic deformation is present. With this in mind, it is hard to describe large displacements and rotations that are found in beams, cables and shells. Such problems require a nonlinear theory which includes the (deformed) geometry in an exact way (Wriggers, 2008).

2.2.3.2 Newton-Raphson method
The Newton-Raphson method is an iteration method commonly used in numerical analysis. It uses equilibrium iterations to avoid accumulation of errors in each load step. The equilibrium iterations are used to establish equilibrium to a desired accuracy at each load step before the solution moves forward. The method applies two steps intermittently: check if equilibrium is satisfied within the desired accuracy, if not, make a suitable adjustment of the state of deformation (Krenk, 2009).

The Newton-Raphson method linearizes the nonlinear functions at a given point, with the aim of minimizing the error in the force balance between the internal and external forces. The nonlinear function is approximated by a Taylor expansion about the given point. All the terms

higher than the linear ones are ignored and the multidimensional nonlinear function is given by the equilibrium equation;

$$\psi(a) = \int_V \boldsymbol{B}^T \boldsymbol{\sigma} dV - \boldsymbol{f} = 0$$

The external forces, $\boldsymbol{f}$, are known while the stresses, $\boldsymbol{\sigma}$, are dependent on the nodal displacement, $\boldsymbol{a}$. If the approximation a^{i-1} has been established as a (preliminary) solution to $\boldsymbol{a}$, then a Taylor expansion of ψ about a^{i-1} provides,

$$\psi(a^i) = \psi(a^{i-1}) + \left(\frac{\partial \psi}{\partial a}\right)^{i-1} \cdot (a^i - a^{i-1})$$

The expression provides the linearized approximation to the true expression for $\psi(a^i)$. This represents the tangent to the curve for the last known state of equilibrium.

By establishing the derivative in the expression, a solution to the equilibrium equation can be found. To proceed further, the derivative of $\partial \psi / \partial a$ needs to be identified. Since the external loading is fixed it is implied that:

$$\left(\frac{\partial \psi}{\partial a}\right) = \int_V B^T \frac{d\sigma}{da} dV$$

Where the constitutive relation $\boldsymbol{\sigma} = \boldsymbol{D}_T \boldsymbol{\varepsilon}$ is used to get:

$$d\sigma = D_t d\epsilon = D_t B da$$

Which gives

$$\frac{d\sigma}{da} = D_t B$$

and the relation $\left(\frac{\partial \psi}{\partial a}\right) = \boldsymbol{K}_t$ gives:

$$\int_V \boldsymbol{B}^T \boldsymbol{D}_t \boldsymbol{B} dV = \boldsymbol{K}_t$$

Where K_T is defined as the tangential stiffness matrix.

The tangential stiffness matrix is calculated for every iteration and is calculated from the last know state of equilibrium. If the first iteration does not reach equilibrium the algorithm is repeated until the equation reaches equilibrium (Ottosen & Ristinmaa, 2005).

2.3 Buckling

Buckling of a column happens when a column is exposed to its critical load. The critical load is defined as the load which is sufficient to keep it in a slightly bent form, i.e. in a deformed

state of equilibrium. Depending on the boundary conditions of the column, the bent form will look different (Timoshenko & Gere, 1961).

First, we consider an ideal column, which is perfectly straight and compressed by an axial load. The column is fixed in the bottom and free at the top. If the load, P, is less than the critical value, the column will only be exposed to axial compression and remain straight. This state is called *a stable state*. A stable state means that if a lateral force is applied and produces small deflections, the deflection disappears when the lateral force is removed and the column returns to its stable, straight form (Timoshenko & Gere, 1961).

If the axial load, P, is gradually increased, an *unstable* form will be reached. This means that a small lateral force will produce a deflection which does not disappear when the lateral force is removed (Timoshenko & Gere, 1961).

The axial load needed for this to happen is called the critical load.

2.3.1 Critical load

There exist several ways to calculate the critical load. The method that will be explained is the Euler buckling formula. To be able to use the formula, two criteria need to be fulfilled: The column needs to be initially straight with the same cross-section along its length and made by a homogeneous material with unlimited elasticity and an initially centric compression force that will keep its direction through the buckling. If these criteria are met, it is possible to use the Euler buckling formula (Pettersson, 1971).

$$P_k = \frac{\pi^2 EI}{(\beta L)^2}$$

To use the formula, the Young's modulus (E) of the material, the moment of inertia (I) dependent on the cross-section, the length (L) of the column and the variable value, β, that is dependent of what type of attachment is used, is needed (Pettersson, 1971).

Euler had four different buckling cases which can be seen in fig.11. Depending on the attachment, the bar will deform differently. The value of β multiplied with the length gives the so-called buckling length (Pettersson, 1971).
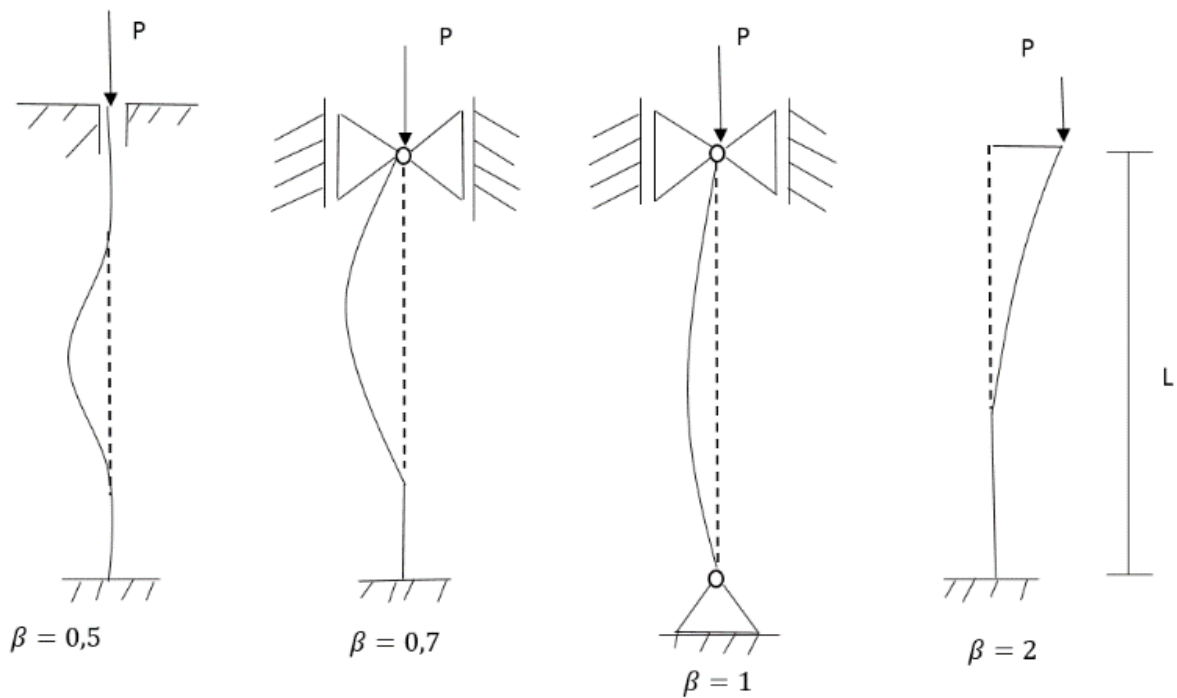
Figure 11. Euler's four different buckling cases where the value of β is based on the attachment of the bar. Adapted from (Pettersson, 1971).

Thus, when a buckling case is known (or assumed to be relevant) the buckling length is also known (or assumed to be relevant) and the critical load can be calculated.

2.3.2 Buckling analysis in Abaqus

When performing a buckling analysis in Abaqus, the software estimates the elastic buckling by eigenvalue extraction. This type of estimation is usually used for "stiff" structures, where the pre-buckling responses are almost linear. The extracted eigenvalue gives a value that represents how many times the applied load can be multiplied before the structure buckles. This way, the structure's critical load can be determined. The buckling analysis in Abaqus can differ from the Euler calculation. Euler's calculation is based on classic beam theory while the finite element model can be based on e.g. a 3D model and in any case a numerical solution is obtained, which means it is not exact. The finite element model results are also heavily dependent on element size (mesh size) and boundary conditions, which can make the result differ.

3 Analysis

3.1 Model

The model in Abaqus was modelled after the "Warehouse" model made in Robot.

3.1.1 Element type

When modelling there is always a decision that has to be made between what element type the model should use to reach a high accuracy while keeping the computing time as short as possible.

The analysis emphasizes on the phenomena that happen in the top-chord of the truss and the CGI-plates. A high accuracy is beneficial for the results on these parts. A buckling analysis and a static analysis were performed on two different types of models of a *HEB 220* beam, one model using solid elements and one model using shell elements. The purpose was to determine if there was any upside using solid elements in the modelling of the top-chord of the truss beam of the warehouse roof. A *HEB*-profile has rounded welds between the flange and the web which possibly could have any effect on the results and behavior of the model. These welds are possible to model using solid elements, but not with shell elements. For the linear analysis, the middle point of each beam was chosen as a measurement point. For this test an evenly distributed vertical load of 1000 N/m^2 was used. The load case can be seen in fig. 12.
For the buckling analysis, the same beam was used but another load case was used for this analysis. The used load case can be seen in fig. 13. The force used was an concentrated force of $1000 N$.

The results of the test are presented in table 2 and the results indicated that there are almost no difference between the two different element types.
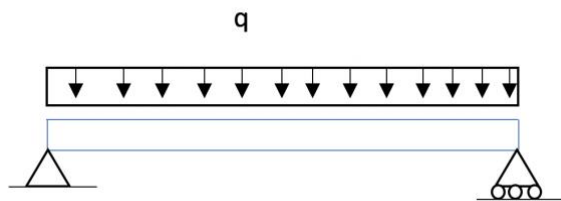
Figure 12. The load case used as for the static analysis.

Figure 13. The load case used for the buckling analysis.

Element type	**Solid**	**Shell**
	Linear analysis	
Y displacement (mm)	65	68
	Buckling analysis	
Eigenvalue 1	94	94
Eigenvalue 2	267	265

The bottom-chord, end-beams and the trusses' webs were modelled with line elements while the CGI-plate were modelled with shell elements. An overview of the elements used for the model in Abaqus can be seen in table 3 and their position can be seen in fig.14.

Table 3. Overview of the elements used for every building element in Abaqus.

Number	**Element**	**Profile**	**Dimension(mm)**	**Length(m)**
1	Colum	HEB	300	10
2	Top-Chord	HEB	220	25
3	Bottom-Chord	HEA	200	20
4	End-Beam	HEA	200	6
5	Web-Vertical	VKR	100×100×5	1,6
6	Web-Diagonal	VKR	100×100×5	2,97
7	Bracing-Horizontal	VKR	100×100×5	6
8	Bracing-Diagonal	VKR	100×100×5	7,81
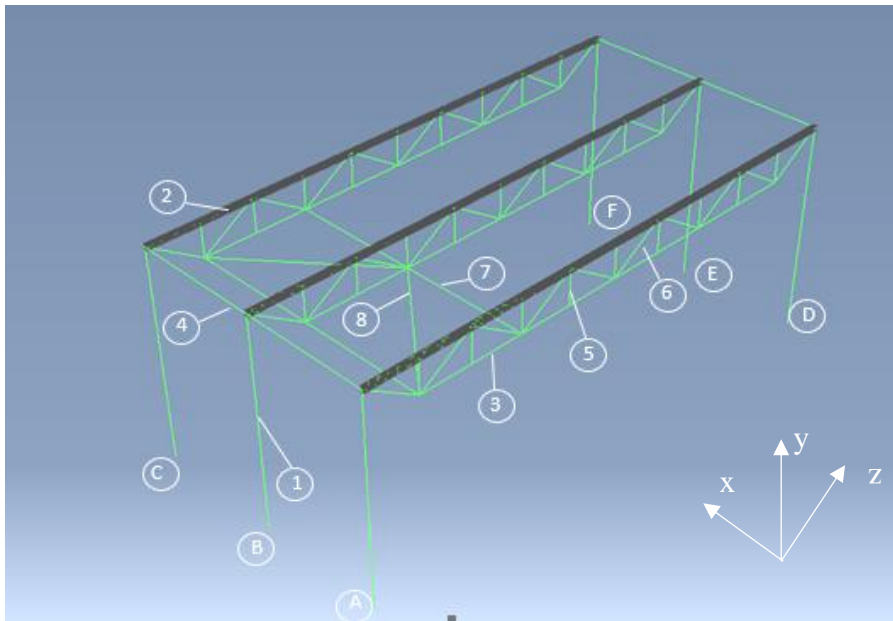
Figure 14. An overview of the warehouse, without its roof, in Abaqus with all its parts numbered.

3.1.2 Material Parameters

The material used for the model an isotropic, linear elastic material, with a Young's modulus of $210 GPa$, representing the S355 material and Poisson's ratio of 0,3.

3.1.3 Mesh

The mesh varies over the building. Different parts have different mesh sizes. The mesh was coarse since the model was large and the analysis did not focus on local phenomena, but more the general stability of the whole building/main girders. Mesh sizes were kept the same through all three models to keep them as close to each other as possible.

3.1.4 Boundary condition

The boundary conditions were designed to resemble columns fixed to the ground. Boundary conditions were put on points A, B, C, D, E and F(fig.12). To resemble a fixed column to the ground in Abaqus, the boundary condition "encastre" was chosen. This option hinders the movement in *X*, *Y* and *Z* direction as well as the rotation around *X*, *Y* and *Z*.

3.1.5 The frame

3.1.5.1 No pillars and end-beams

Since a simple model was searched, it was decided to analyze if the end-beams and columns were necessary for the forthcoming analysis. A linear analysis and a non-linear analysis were performed to determine what differences it would make to remove said end-beams and

19

columns. The applied load consisted of a vertical load of $1000 N/m^2$ that was distributed uniformly over the structure. The result from the linear analysis can be found in table 4 and results from the non-linear analysis can be found in table 5. The result from the model with pillars act as a reference. The result from the model without pillars shows the difference between the two in millimeters. If the value is negative, it means that the value is smaller than the reference value.

The analysis showed that the model without columns had a larger deformation in Y and X direction in both the linear and non-linear cases. Since the difference is fairly small between the two models, it was decided to move on with the Modell without end-beams and columns.

Table 4. Result from the linear analysis.

Model	P-1	P-2	P-3	P-4	P-5	P-6	P-7
Displacement mm	Y	Y	Y	Y	Y	X	X
Pillars	ref	ref	ref	ref	ref	ref	ref
No-pillars	0,062	0,064	0,66	-0,22	0,66	1,8	1,7

Table 5. Results from the non-linear analysis.

Model	P-1	P-2	P-3	P-4	P-5	P-6	P-7
Displacement mm	Y	Y	Y	Y	Y	X	X
Pillars	ref	ref	ref	ref	ref	ref	ref
No-pillars	0,012	0,015	1,96	-0,94	1,96	6,20	6,02

3.1.5.2 Modified model

The frame of the model consists of three trusses with a bracing, located on side B (as seen in fig.15), between the trusses. Each truss consists of a top-Chord, bottom-chord and web members (vertical and diagonal). The web members are connected with a rigid connection to the top and bottom chord. The truss connections are emulating a truss that is welded together.
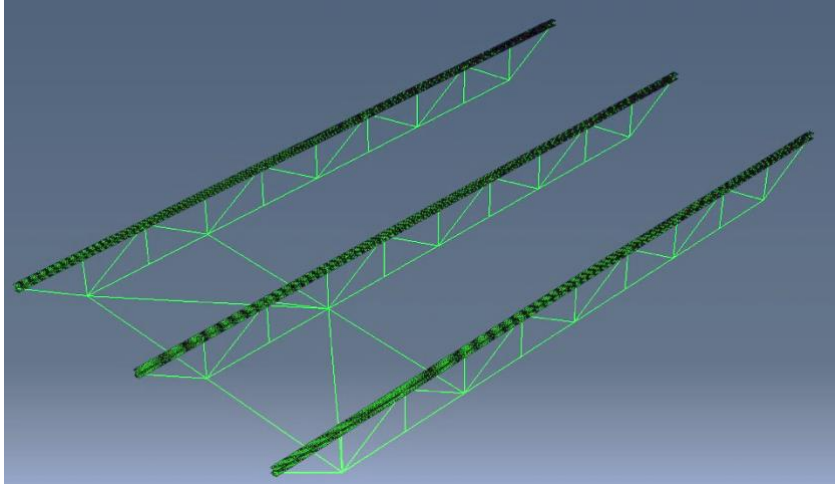
Figure 15. The frame used for the model.

The bracing acts as a support for the bottom-chord. A closer look of the bracing can be seen in fig.16.
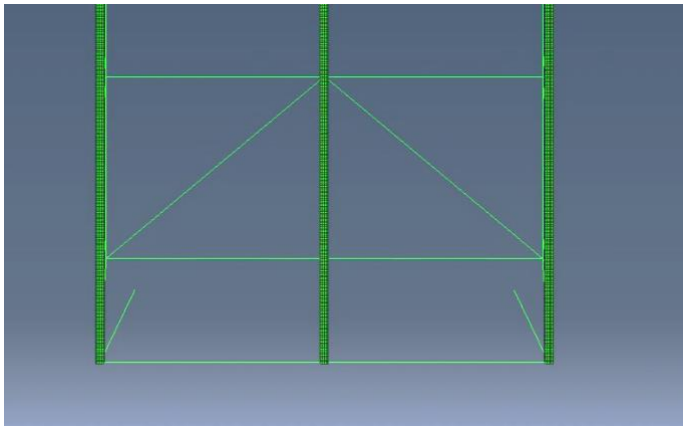
Figure 16. A closer look of the bracing used.

3.1.5.3 Modified boundary conditions

When the columns and end-beams where taken out from the model, new boundary conditions had to be assigned, since the old ones where located on the column. The boundary condition would be located on the top-chords and had to allow rotation around X, Y and Z. One side of the building (P-11, P-12 and P-13) would have to be fixed in X, Y and Z direction while the other side (P-14, P-15 and P-16) had to be fixed in X and Y, to allow movement of the top chords in Z direction. An overview of the boundary condition can be seen in table 6 and their location can be seen in fig.17.
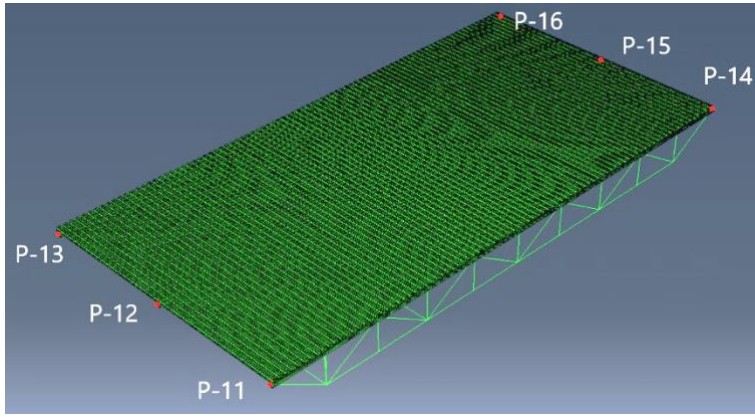
Figure 17. an overview of the locations of the boundary conditions.

Table 6. The boundary conditions used for the analyzed models.

Point	U1	U2	U3
P-11	√	√	√
P-12	√	√	√
P-13	√	√	√
P-14	√	√	-
P-15	√	√	-
P-16	√	√	-

3.1.6 Multi-point constraint

When using shell elements as beams and applying the boundary condition on the lower flange, there is a risk for a local buckling occurring in the web. To counteract this, and to create a possibility to only use one point for the boundary condition, a *Multi-point constraint* was created. As the name implies, multiple points (nodes) act as slaves, and one-point acts as a master (control point). The slave nodes will follow the master node's in rotation and displacement as if they were rigidly connected to the master node. An illustration of this is seen in fig.18.
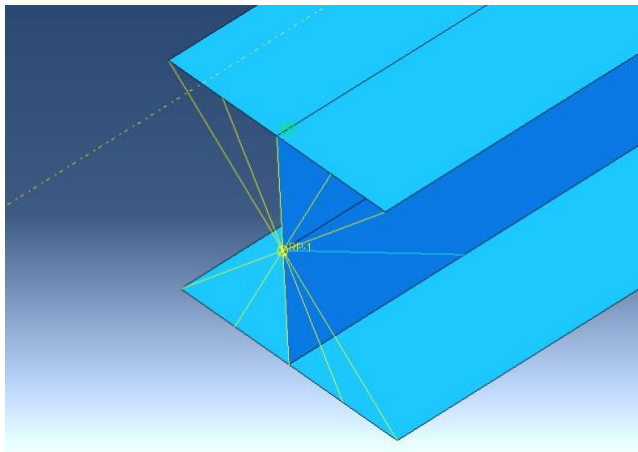
Figure 18. The point RP-1, acts as an master node. The yellow strings are an illustration of the slave nodes connection to the master.

22

3.1.7 Surface-based constraint

For the connection between the truss elements, surface-based constraints are used. To connect the truss components (Top-chord, webs and Bottom-chord) to each other, a tie constraint was used. The tie constraint works similarly to the MPC, one surface/node group is the master and the other one is the slave. In the model, when a web connects to the top-chord, the top chord acts as master and when connected to the bottom-chord the bottom-chord acts as master (fig.19). Both points of the web act as slaves. The degrees of freedom can be chosen for each instant. In this model all the tie constraints are rigid.
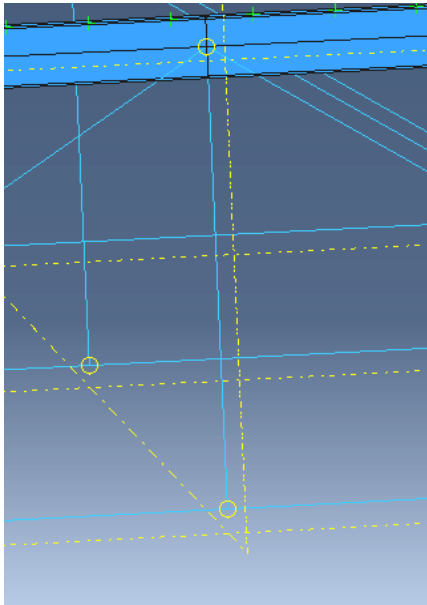
Figure 19. An tie connection for the truss in the model.

3.1.8 Roof

Three variations of roof-modelling were explored to understand how much the modelling of the roof affects the result and to gain knowledge how these types of roofs should be modeled. The profile of each roof type is always the same and based on the technical drawing provided by Rukki (appendix A).

Model A is composed of 60 CGI plates with the dimensions $0.840 \cdot 6.22$ m. This model is the most complex of the three and is an accurate representation (visually) of how this type of building is constructed in reality. Since there are several CGI plates in this model, an overlap of the CGI plates in direction *Z* and in direction *X* has to be modelled. A model of the roof can be seen in fig.20.
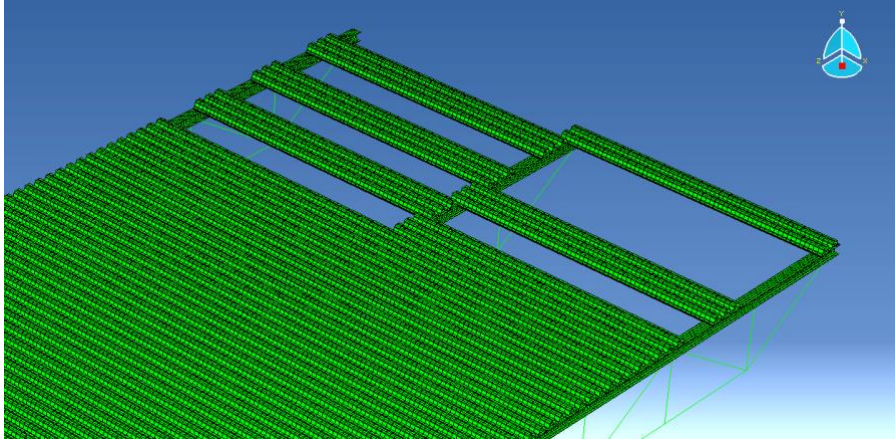
Figure 20. An illustration of how the CGI-plates are connected in model A.

Model B is composed of two CGI plates with the dimensions $25 \cdot 6.22$ m . The overlap between the CGI plates horizontally in direction X is non-existent in this model while the overlap in Z direction, at the middle top-chord is still considered. Since the interaction between two elements is one of the toughest challenges when modeling, fewer interactions in a model is usually preferred, making this model much easier to handle than model A. One of the two CGI plates that act as this model's roof can be seen in fig.21.
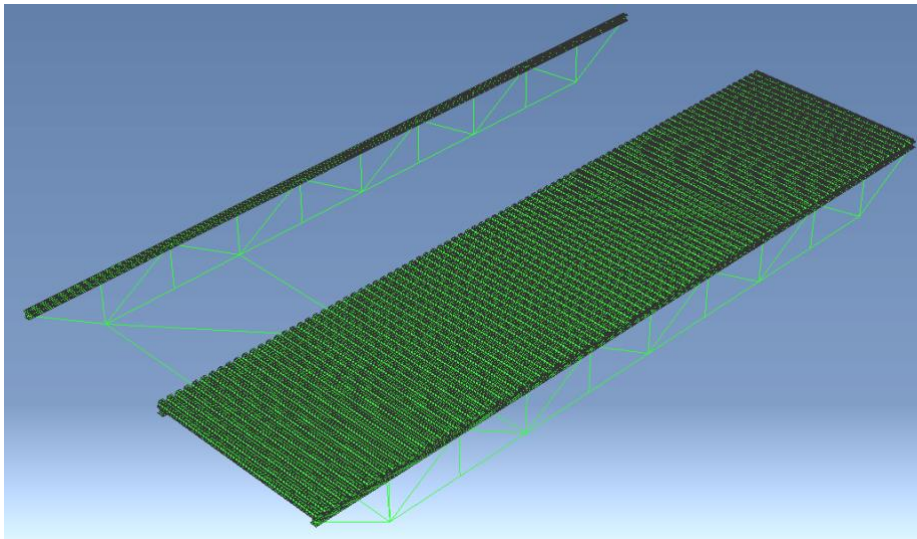
Figure 21. An illustration of Model B and its two CGI plates.

Model C is composed of one CGI plate with the dimension $25 \cdot 12$ m . This model does not have any interaction between different CGI plates, and is the simplest model of the three. The roof can be seen in fig.22.
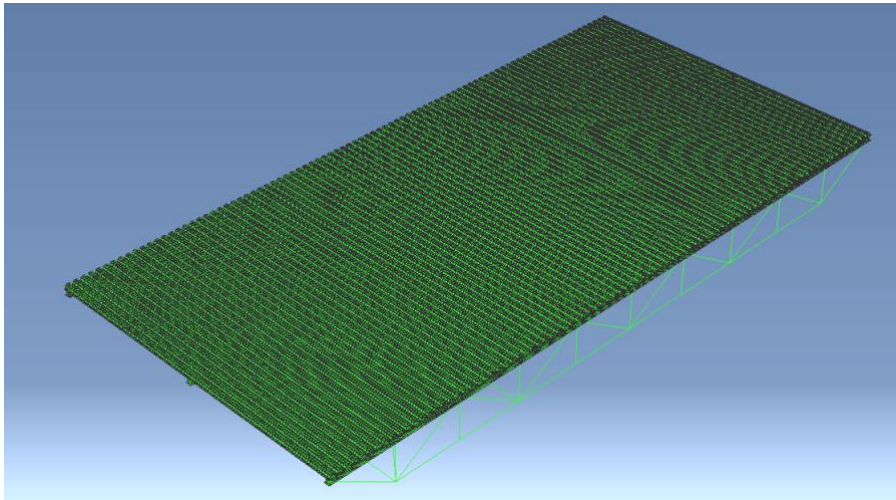
Figure 22. The roof of model C.

3.1.9 Connectors

A connection between the CGI plates and top chords had to be established. According to the technical drawings provided by *Rukki* (*Appendix A*) the elements are connected with screws with a spacing of $0,280$m in direction Z. To simulate a screw connection in Abaqus, a fastener called "spot-weld" was used. This fastener simulates a spot-weld between two elements where the radius (area) of the spot weld and the rigidity of the connector can be modified by the user. The connector elasticity was rigid during the analysis and then changed in the parametric study. The radius of the spot-weld was kept the same trough out the simulations. An illustration of how this is presented in Abaqus can be seen in fig.23.
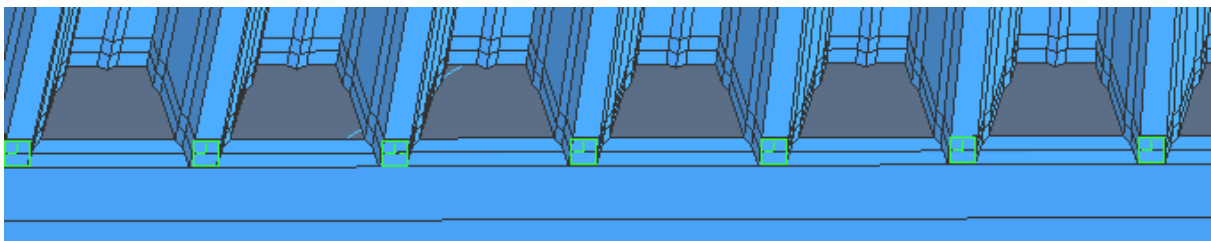
Figure 23. Spot-weld fastener with a distance of 0,280 m.

For model A, additional fasteners were used in the *X* direction to connect the CGI-plates to each other. The distance between the fasteners are 0,500m and can be seen in fig.24.
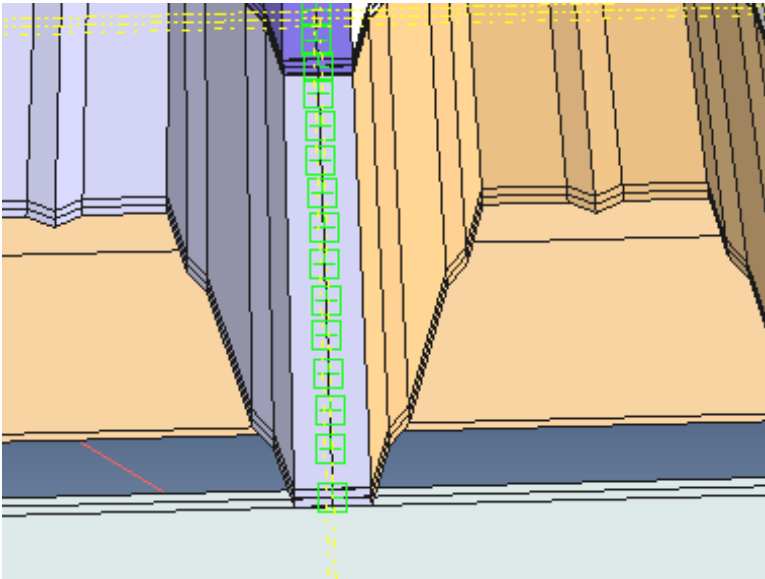
Figure 24. Fasteners used to connect the CGI-plates to each other in model A.

3.1.10 Load

For the linear-static and linear-buckling analysis, the load used was 1000N/m^2. Since the profile of the CGI-plates is not plane, but profiled, the steel area is larger than the vertical projection of the roof area, which is $25 * 12 = 300\text{m}^2$ while the steel area is 1,8 times bigger. To get the correct total force, i.e. representing the total vertical load per horizontal roof area, all the loads needs to be scaled down 1,8 times in *Abaqus*. Fig. 25 demonstrates the ratio. The distance S is 1,8 times the distance L.
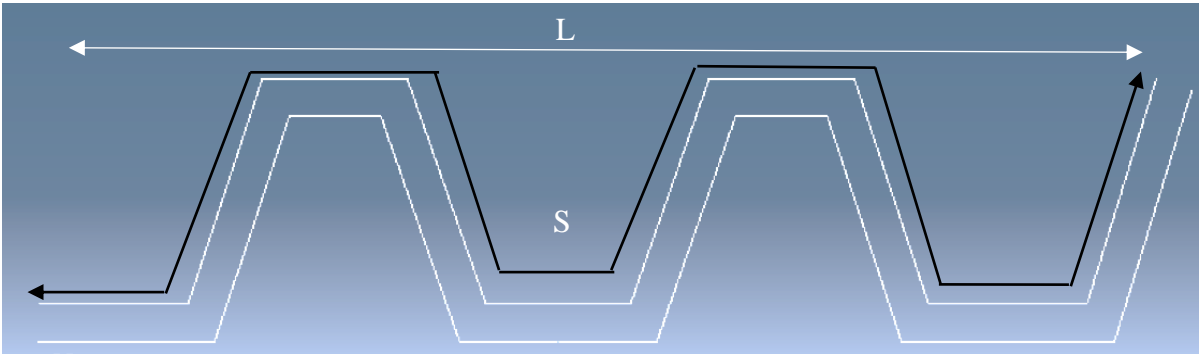
Figure 25. S=1,8L

The warehouse is exposed to a dead load (a combination of roof weight and installations), snow load and wind load. As it is unlikely that the snow and wind will reach extreme values at the same time, two different load cases were tested, one with snow as leading action and one with wind as leading action, where, as it turned out, suction on the roof was the interesting part.

The magnitudes of the loads are based on Eurocodes.

Load case 1 – Snow load leading

$Sk = 1500\text{N/m}^2$
$\mu = 0,8$
$C_e = 1$
$C_t = 1$

$Snow\ load(SL) = 0,8 \cdot 1500 \cdot 1 \cdot 1 = 1200\text{N/m}^2$

$Deadload(DL) = 1000\text{N/m}^2$

Reliability class 3
$y_d = 1$

Permanent load
$y_d \cdot 1200 \cdot DL = 1200\text{N/m}^2$

Leading action
$y_d \cdot 1500 \cdot SL = 1 \cdot 1500 \cdot 1,2 = 1800\text{N/m}^2$

Total load

$1200 + 1800 = 3000\text{N/m}^2$

Load case 2 – Wind load leading (suction)

$Deadload\ (DL) = 1000\text{N/m}^2$

$Basic\ wind\ velocity(vb) = 26\ \text{m/s}$
$Terrain\ category = 2$
$Height = 10\text{m}$
$q_k = 910\text{N/m}^2$
$cpe,_{10} = -0,7$
$cpi,_{10} = 0,3$

30 % of the characteristic wind pressure will create suction on the roof

$Windload(w_e) = 910 \cdot (-0,7 - 0,3) = -910\text{N/m}^2$

Reliability class 3

$y_d = 1$

Permanent load (favorable)

$0{,}9 \cdot DL = 900\text{N/m}^2$

Leading action
$1 \cdot 1{,}5 \cdot (-910) = -1365\text{N/m}^2$

Total load

$0{,}9 - 1365 = -465\text{N/m}^2$

3.2 Performed analyses

3.2.1 Linear static analysis

The study of the different roof types was performed through a linear static analysis (small displacement theory). Displacement in vertical and horizontal direction were examined, as well as the force distribution (support reactions). Linear static analysis is one of the simpler analyses available in Abaqus and is one of the less time-consuming analyses. This analysis step also worked as a way to control that the model was working correctly.

Thirteen points on the model were chosen for output. Five of these were for observation of displacement in the vertical direction, two were for displacements in the horizontal direction and six were for the observation of force distribution. Their name and location can be seen in figs.26, 27 and 28.
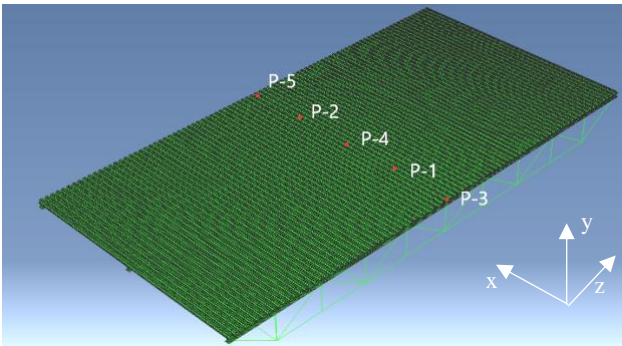
Figure 26. The five points used for the vertical reading.
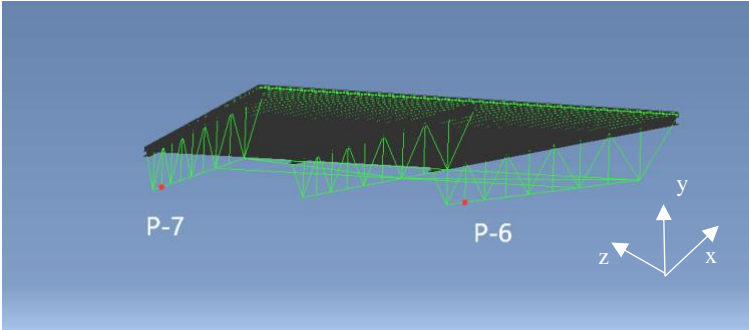
Figure 27. two points used for the horizontal reading.
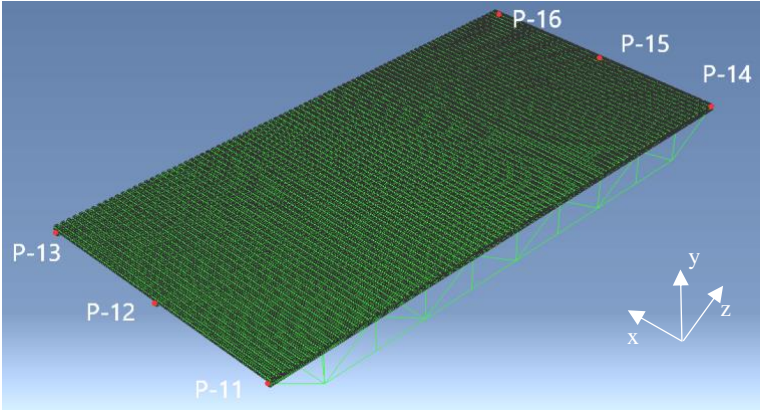
Figure 28. The six points used for the load distribution reading.

3.2.2 Non-Linear static analysis

The non-linear analysis was used to better understand the behavior of the roof during the application of the load, and to examine if the behavior is different when nonlinearity is considered. The non-linear analysis will, as the static analysis, focus on vertical displacements, horizontal displacements and force distribution.

Initially the non-linear analysis would not converge for models B and C. The outer flanges of these models buckled during the analysis and it was decided to test thicker outer flanges to see if the model would converge, since the result pointed to a stability problem in that part of the building. Thickness of the outer flanges, as seen in fig. 29 was changed on all the models to $3\ mm$ to keep the continuity between the models. This helped with the convergence and stability issue.
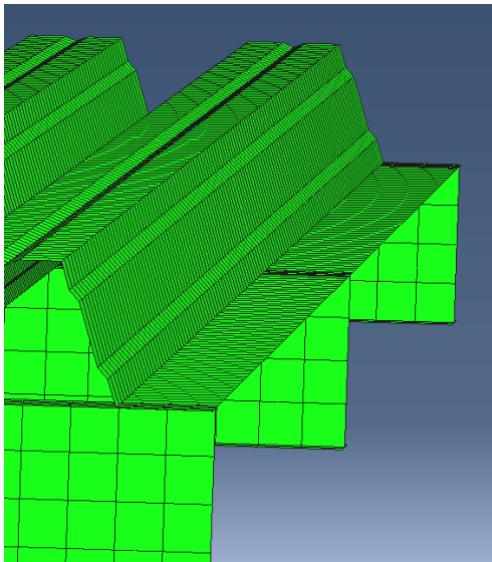
Figure 29. the outer flange which needed to be made thicker to obtain converged solutions.

The second test with the linear static analysis and the non-linear analysis showed an load distribution in model A and B that was equal to a load distribution that would occur in a simply supported beam, meaning the middle truss would support 50 % of the load and the outer trusses would support 25 % of the load each. Since model C was modelled with one continuous CGI-plate, its load distribution resembled an model with a continuous sheathing, meaning its middle truss would support 60% of the load and the outer trusses would support 20 % of the load each. All three models needed to behave the same, to be able to compare the results against each other. The CGI plates on model A and B were then spot-welded together according to technical drawing in *appendix A* and new tests were made with the new models. The additional spot-weld can be seen in fig.30. This additional spot-welding made the three to behave the same and the test could move forward.
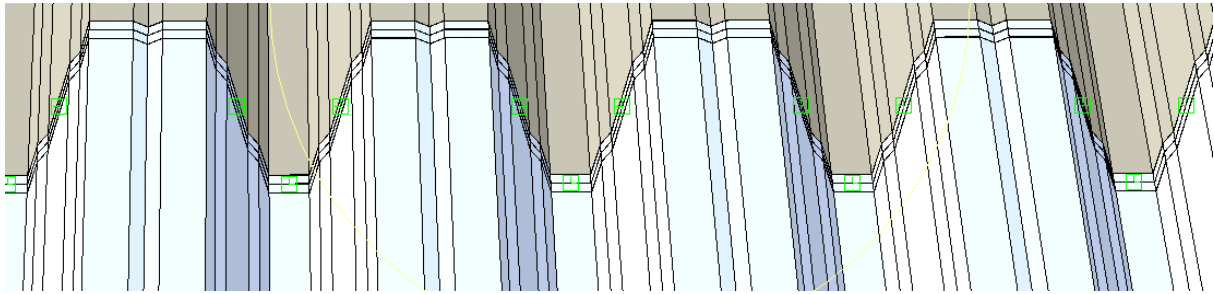
Figure 30. The additional spot-welding based on drawing from Appendix A.

After the linear and non-linear analysis, it was decided to only move on with Model B. The difference between the roof types result was small enough to only move on with one of the models. Model B was used as a reference model for further parametric studies since its values were between model A and model C, and one can assume the real values are somewhere in-between A and C.

3.2.3 Buckling analysis

A buckling analysis tells the user how much force is needed for the model to buckle. Through visualization, Abaqus shows the user the buckling mode (the shape of the deformed state of equilibrium) for each mode the user has requested. The buckling analyses were performed only on model B. The result showed that the bottom chord would buckle, which can be seen in fig.31, when exposed to a load of -2360N/m^2, which is approx. 5,5 times bigger than the applied load of -465N/m^2.
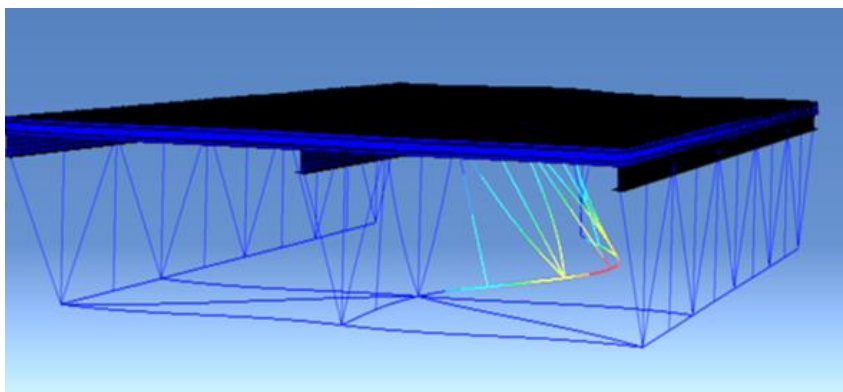
Figure 31. The buckling of the bottom-chord.

3.2.4 Non-linear buckling analysis

A type of non-linear buckling analysis was performed to examine if the buckling behavior would change and to compare the two buckling analyses.

There are two different approaches to perform non-linear buckling analyses in Abaqus. One approach is to use the general Riks method (also called the "arc length" method), which can be used, e.g. to follow unstable so-called snap-back behavior. Another approach is to add a buckling step after a non-linear static step, which is a means to include nonlinearities at lower load levels which might be of importance in the estimation of the buckling load at higher load levels. Different force-discplacments behavior can be seen in fig.32.

The method used in the analysis was the adding of a buckling step after the non-linear analysis. Note that this approach does not include the ability to track snap-back problems.
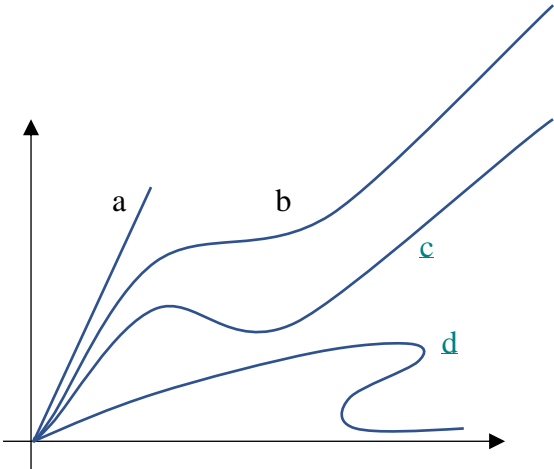
Figure 32. showing the different force-displacement behaviors a, linear b, nonlinear(monotonic increase) c, nonlinear (with local minimum) and d, general nonlinear behavior including snap-back.

3.2.3.1 Different nonlinearities

It is usually assumed that for each load step, the load is increased by a certain amount and then held constant during the iterations. This assumption works fine when the displacement increases with the load level. In reality, not every structure will respond this way. For example, some structures have a softening response when their peak load is reached. This means that the earlier assumption, when assumed wrong, will make the equilibrium equations continue forever, since the softening branch would not be able to be traced correctly. An example is shown in fig.33.
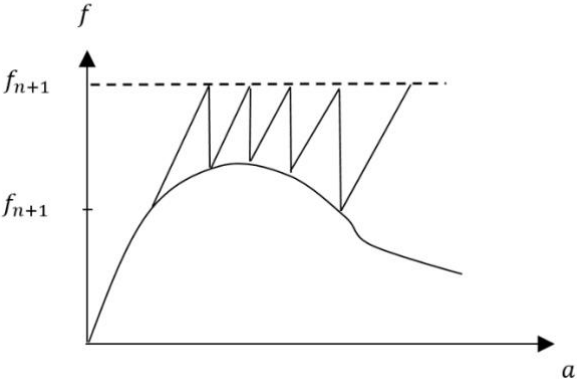
Figure 33. Displaying an softening response after peak load. When the load $f_{(n+1)}$ is held constant, the equilibrium equations would continue forever since the softening branch would not be traced correctly. Adapted from (Ottosen & Ristinmaa, 2005).

32

The peak load is always interesting for an engineer and it is often argued that when the equilibrium equations do not converge, the peak load has been reached. This way of thinking can be dangerous since equilibrium iterations may diverge for a number of reasons. Important information, regarding ductility or brittleness of the structure, can be missed if the descending branch is not traced after peak load. Fig.34 illustrates a ductile and brittle response of a structure as well as the phenomenon called *snap-back.*
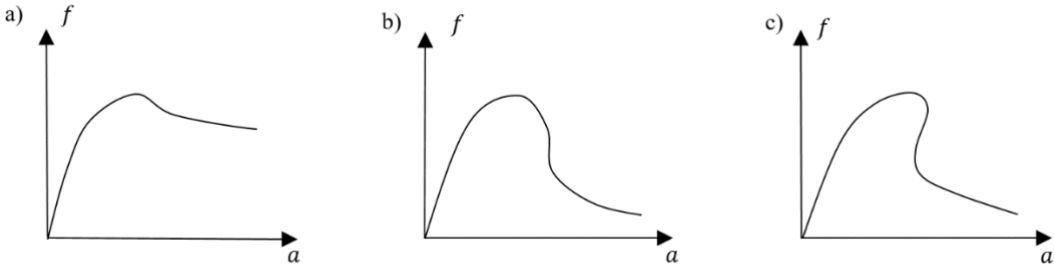
Figure 34. a, Ductile response. b, Brittle response. c, The snap-back phenomenon. Adapted from (Ottosen & Ristinmaa, 2005).

The strategies used to trace the various post-peak responses are called path-following methods. The Riks-method is one of the methods that can be used for problems like these.

The method, when used in Abaqus, uses the load magnitude as an additional unknown and solves it simultaneously. Thus, another quantity has to be used to measure the progress of the solution. Abaqus uses "the arc-length", hence its name, along the static equilibrium path in load-displacement space. With this approach it is possible to present results regardless if the response is stable or unstable (Sharcnet, u.d.). Fig. 35 shows a typical snap-trough situation which can be encountered when buckling analysis are used.
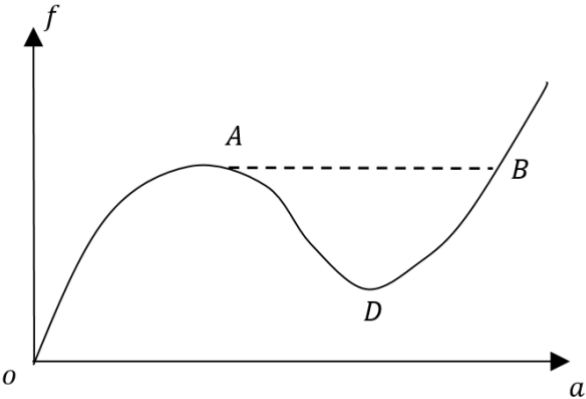
Figure 35. If the arc-length method wouldn't be used in this case the information after point A would be lost. Adapted from (Ottosen & Ristinmaa, 2005).

3.2.5 Parametric study

To gain more knowledge of the model and what affects deformation and buckling on a structure like the one studied, two parametric tests were performed.

Connector elasticity

Different connector elasticities were tested to determine what type of effect the stiffness of the fastener has on the displacement, the force distribution and the buckling. The stiffness in all directions were changed simultaneously.

The tried stiffnesses were $10^6, 10^7$ and $10^9 \ N/m$. Linear, non-linear and buckling analyses were performed. A stiffness value below $10^6 \ N/m$ resulted in non-convergence since the connectors were so flexible that the model fell apart.

CGI-sheet thickness

To understand what impact the thickness had on the displacement and buckling, a parametric study was made where different thicknesses $(0.4, 1.6 \text{ and } 3.2 \ mm)$ were used while doing a linear/non-linear static analysis and a buckling analysis. When the thickness of 0.4 mm was used, convergence could not be found since the thin CGI-plate did not have enough stiffness to not buckle before the complete load was applied.

4 Results

The results are presented in such way that one value will act as a reference value. The other values are presented only with the difference between itself and the reference value in percent.

4.1 Linear static analysis

Table 7. The results from the linear static analysis where the load $1 kN/m^2$ was used.

Model	P-1	P-2	P-3	P-4	P-5	P-6	P-7
Displacement difference %	Y	Y	Y	Y	Y	X	X
A	ref	ref	ref	ref	ref	ref	ref
B	2,11	2,10	-0,13	0,11	-0,14	8,13	8,41
C	1,93	1,90	-0,44	0,38	-0,45	8	8,10

Table 8. Result from the force distribution that shows the force distribution In the models.

Model	P-11	P-12	P-13	P-14	P-15	P-16
Force Distribution %	RF in Y	RF in Y	RF in Y	RF in Y	RF in Y	RF in Y
A	10	29	10	11	29	11
B	10	29	10	11	29	11
C	10	29	10	11	29	11

4.2 Non-Linear static analysis

4.2.1 Load case A

Table 9. Result from the Non-linear static analysis when load case A was used.

Model	P-1	P-2	P-3	P-4	P-5	P-6	P-7
Displacement difference %	Y	Y	Y	Y	Y	X	X
A	ref	ref	ref	ref	ref	ref	ref
B	2,0	2,0	-0,3	0,2	-0,3	13,5	13,9
C	2,1	2,1	-0,5	0,4	-0,5	14,2	14,2

Table 10. Force distribution for the three models during the non-linear analysis with load case B.

Model	P-11	P-12	P-13	P-14	P-15	P-16
Force Distribution %	RF in Y	RF in Y	RF in Y	RF in Y	RF in Y	RF in Y
A	10	29	10	11	29	11
B	10	29	10	11	29	11
C	10	29	10	11	29	11

4.2.2 Load case B

Table 11. Result from the Non-linear static analysis when load case B was used.

Model	**P-1**	**P-2**	**P-3**	**P-4**	**P-5**	**P-6**	**P-7**
Displacement difference %	*Y*	*Y*	*Y*	*Y*	*Y*	*X*	*X*
A	ref	ref	ref	ref	ref	ref	ref
B	2,1	2,1	-0,1	0,1	-0,1	6,3	6,6
C	1,9	1,9	-0,4	0,4	-0,4	6,1	6,2

Table 12. force distribution for the three models during the non-linear analysis with load case B.

Model	**P-11**	**P-12**	**P-13**	**P-14**	**P-15**	**P-16**
Force Distribution %	*RF in Y*	*RF in Y*	*RF in Y*	*RF in Y*	*RF in Y*	*RF in Y*
A	10	29	10	11	29	11
B	10	29	10	11	29	11
C	10	29	10	11	29	11

4.3 Buckling analysis

Table 13. The eigenvalues from the buckling analysis. A negative value means that the parts buckle when the load is applied the reversed direction, in this case, on the inside of the roof.

Mode	1	2	3	4	5	6
Part	*Outer flange*	*Outer flange*	*Bottom chord*	*Bottom chord*	*Outer flange*	*Outer flange*
Applied load	1000	1000	1000	1000	1000	1000
Eigenvalue	2,32	2,42	-2,46	-2,74	-2,78	-2,80
Buckling load	2320	2420	-2460	-2740	-2780	-2800
% of load case 1 or 2	77	80	530	590	588	600

4.4 Non-linear buckling analysis

Table 14. The eigenvalues from the buckling analysis.

Mode	1	2	3	4	5	6
Part	*Bottom chord*	*Bottom chord*	*Outer flange*	*Outer flange*	*Outer flange*	*Outer flange*
Applied load	-465	-465	-465	-465	-465	-465
Eigenvalue	4,39	5,43	-5,59	-5,69	-7,02	-7,13
Buckling load	-2460	-2526	2598	2644	3263	3316
% of load case 1 or 2	530	543	86	88	108	110

4.5 Parametric study

4.5.1 Connector stiffness

Table 15. Result from the Linear analysis made on Model B where three different stiffnesses on the connectors where tested.

Linear static	P-1	P-2	P-3	P-4	P-5	P-6	P-7
Displacement difference %	Y	Y	Y	Y	Y	X	X
Rigid	ref	ref	ref	ref	ref	ref	ref
1e9	2,7	2,7	-1,0	0,9	-1,0	-89,4	-89,5
1e7	17,7	17,7	8,3	-7,0	8,3	-70,9	-61,8
1e6	32,1	31,6	13,3	-12,2	14,2	-70,2	-56,2

Table 16. The force distribution for the three test when a linear analysis is made.

Linear	P-11	P-12	P-13	P-14	P-15	P-16
Force Distribution %	RF in Y	RF in Y	RF in Y	RF in Y	RF in Y	RF in Y
Rigid	10	29	10	11	29	11
1e9	10	29	10	11	29	11
1e7	12	27	12	12	26	12
1e6	13	25	13	13	24	13

Non-Linear

Table 17. Result from the non-linear analysis made on Model B where three different stiffnesses on the connectors where tested.

Non-Linear	P-1	P-2	P-3	P-4	P-5	P-6	P-7
Displacement difference %	Y	Y	Y	Y	Y	X	X
Rigid	ref	ref	ref	ref	ref	ref	ref
1e9	5,2	5,2	-1,1	1,1	-1,1	-95,0	-95,5
1e7	20,7	20,7	8,2	-6,8	8,2	-92,0	-85,3
1e6	35,4	35,0	14,1	-12,0	14,1	-87,8	-81,1

Table 18. The force distribution for the three test during the non-linear analysis.

Non-linear	P-11	P-12	P-13	P-14	P-15	P-16
Force Distribution %	Y	Y	Y	Y	X	X
Rigid	10	29	10	11	29	11
1e9	10	30	10	11	29	11
1e7	12	27	12	12	26	12
1e6	13	25	13	13	24	13

Table 19. Result from the buckling analysis on Model B. The Results in parenthesis are non-comparable.

Buckling	1	2	3	4	5	6
	eigenvalue	*eigenvalue*	*eigenvalue*	*eigenvalue*	*eigenvalue*	*eigenvalue*
Part	Outer flange	Outer flange	Bottom chord	Bottom chord	Outer flange	Outer flange
Rigid	2,32	2,42	**-2,46**	-2,74	-2,78	-2,80
Part	Outer flange	Outer flange	Outer flange	Outer flange	Outer flange	Outer flange
1e9	(1,28)	(1,47)	(-1,48)	(-1,48)	(-1,49)	(-1,49)
Part	Outer flange	Outer flange	Outer flange	Outer flange	Outer flange	Outer flange
1e7	(-1,03)	(-1,04)	(-1,12)	(-1,13)	(-1,77)	(-1,78)
Part	Outer flange	Outer flange	Outer flange	Outer flange	Outer flange	Outer flange
1e6	(-0,76)	(-0,76)	(-0,78)	(-0,79)	(-1,20)	(-1,26)

4.5.2 CGI-Thickness

Linear analysis

Table 20. Result from the Linear analysis made on Model B where three different thicknesses on the CGI-plates where tested.

Linear static	P-1	P-2	P-3	P-4	P-5	P-6	P-7
Displacement difference %	Y	Y	Y	Y	Y	X	X
0,8	ref	ref	ref	ref	ref	ref	ref
1,6	-16,90	-16,90	6,4	-5,64	6,4	-36,3	-36,2
3,2	-27,0	-27,0	14,3	-12,43	14,3	-59,8	-59,8

Table 21. the force distribution following the linear test.

Linear	P-11	P-12	P-13	P-14	P-15	P-16
Force Distribution %	RF in Y	RF in Y	RF in Y	RF in Y	RF in Y	RF in Y
0,8	10	29	10	11	29	11
1,6	11	29	11	11	28	11
3,2	11	28	11	11	28	11

Non-linear analysis

Table 22. Result from the Linear analysis made on Model B where three different thicknesses on the CGI-plates where tested.

Non-Linear	P-1	P-2	P-3	P-4	P-5	P-6	P-7
Displacement Difference %	Y	Y	Y	Y	Y	X	X
0,8	ref	ref	ref	ref	ref	ref	ref
1,6	-17,4	-17,4	7,2	-6,4	7,2	-39,7	-39,5
3,2	-27,6	-27,6	15,2	-13,4	15,2	-63,5	-63,5

Table 23. The force distribution following the non-linear test.

Non-linear	P-11	P-12	P-13	P-14	P-15	P-16
Force Distribution %	*RF in Y*	*RF in Y*	*RF in Y*	*RF in Y*	*RF in Y*	*RF in Y*
0,8	10	29	10	11	29	11
1,6	11	29	11	11	28	11
3,2	11	28	11	11	28	11

Buckling

Table 24. Result from the buckling analysis when the thickness is changed. The results in parenthesis are non-comparable.

Buckling	1	2	3	4	5	6
	Eigenvalue	*Eigenvalue*	*Eigenvalue*	*Eigenvalue*	*Eigenvalue*	*Eigenvalue*
Part	Outer flange	Outer flange	Bottom chord	Bottom chord	Outer flange	Outer flange
0,8	(2,32)	(2,42)	**-2,46**	(-2,74)	(-2,78)	(-2,80)
Part	Bottom chord	Bottom chord	Outer flange	Outer flange	Outer flange	Outer flange
1,6	**-2,55**	(-3,08)	(-4,20)	(-4,20)	(-4,20)	(-4,20)
Part	Bottom chord	Bottom chord	Outer flange	Outer flange	Outer flange	Outer flange
3,2	**-2,67**	(-3,22)	(-4,40)	(-4,40)	(-4,40)	(-4,40)

5. Discussion

5.1 Results

5.1.1 Linear static analysis
The displacement difference was minimal between *model B* and *model C* with the largest percentage difference being 0.32 %. When comparing model *A* and model *B,* the vertical displacement difference was smaller than the horizontal difference. An explanation for this could be that the overlap between CGI-sheets in direction X affects the model. The horizontal displacement can also be affected by the $60\ mm$ outer flange on model *A,* while the outer flange is $80\ mm$ in model *B* and *C.* The difference between the displacement is still small enough ($0.60\ mm$) to consider it as negligible when performing a linear analysis.

5.1.2 Non-linear static analysis

Non-linear – Load case 1
Results from the non-linear analysis are similar to the linear analysis. The difference in displacement in vertical direction is still very similar between model B and C, where the largest percentage difference between the displacements is 0.3%. The largest difference in vertical displacement occurs on the CGI-plate between model *C* and *A*.

Displacement difference in horizontal direction is also larger in the non-linear analysis. In the bottom-chord, there is a difference between model C and A of approximately 14 %, which is approx. 2 mm difference.

Non-linear – Load case 2
When load case 2 is analyzed with a non-linear analysis, it is concluded that the behavior of the three models is almost the same as load case 1. The largest vertical difference can again be found in the CGI-plate and the difference is again approx. 2 % larger displacement in models B/C than model A.

The displacement difference is again a bit larger in the horizontal direction, around 6 %, which is the equivalent of 0.2 mm.

Conclusion
Force distribution does not vary between the models or between the analyses. The middle-chord carries 60 % of the load distributed over 2 columns while the outer top-chord carries 40 % of the load together over 4 columns. The variation of displacement among the models is minimal in the examined points. Based on these results, a CGI-sheet roof can be modeled as one continuous sheet. The differences are so small between the different models that it is recommended in future work to use the roof modeling used in model B or model C. Since the difference between the models where so small, the rest of the analysis's are done with only model B.

5.1.3 Buckling analysis
The buckling analysis shows that the first part to buckle on the model will be one of the outer flanges of the CGI-plates. This buckling will happen when approx. 77 % of load case A is

applied to the model. This type of buckling is not important to the study since it does not affect the overall stability of the model, it is a local problem. The outer flanges of the CGI plate are also probably supported way more in reality then what they are in this model, which makes this part hard to buckle in reality.

The analysis showed that the bottom-chord is the first element that buckles. The buckling load is -2460N/m^2 which is approx. 5.5 times bigger then load case 2.

5.1.4 Non-linear buckling analysis

The non-linear analysis gave the same results as the linear-buckling analysis. The only difference between the two analyses was that the first two modes of CGI buckling disappeared, and that the second mode showed buckling in the bottom-chord. Before the buckling step occurs, the structure has already non-linearly deformed with a load of 465N/m2. because of this, the eigenvalue in this step is 4,4 instead of 5,5, but the force needed for buckle is still the same since $1995 + 465 = 2460\text{N/m}^2$ which is the same buckling load as for the linear buckling analysis.

5.1.5 Parametric study

Connector stiffness

The stiffness of the connection will affect the displacements in all directions. In the linear analysis the results show that the vertical displacement changes are not that drastic and unpredictable. With less stiffness in the fasteners, the bigger the displacement in vertical direction. When the connectors are less stiff, the displacement on the middle top-chord(*P-4*) reduces while the displacement on the outer top-chords (*P-4* and *P-6*) increase. This phenomenon occurs because the force distribution changes. Less stiff connectors transform the system from a "continuous" beam to two separated beams. The force distribution can attest to this. With less stiff connectors, the outer top-chord carries 3 % more force than a system with rigid fasteners.

The horizontal displacement decreases when there is a stiffness change. Since the CGI plates are free, they can deform more vertically without affecting the outer top-chord. That's why the horizontal deformation decreases with a stiffness change.

In the non-linear analysis, it is evident that a rigid connection gives a larger horizontal displacement than a elastic connection. A more elastic connections gives the CGI-plates more room to move over the top-chord and thus, the bottom-chord is affected to a lesser degree.

The buckling analysis was performed to investigate what impact the connector stiffness would have on the buckling modes and eigenvalue. When the stiffness in the connector was lowered, the buckling of the bottom-chord disappeared. The result from the buckling analysis with elastic connectors is not comparable to the buckling analysis with rigid connectors. The eigenvalue from the analysis with elastic connectors (results in parenthesis in table 19) can only be compared to each other and not to the result from the analysis with ridged connections, since the buckling mode are different. Buckling occurred exclusively in the CGI-plates when the stiffness was changed. Since the top-chords are given less stabilization when the stiffness in the connectors are lowered, it is possible that buckling in the top-chord would occur in later modes.

One can also assume that a less rigid structure is less likely to buckle since its parts has more room to move.

Conclusion

Connector stiffness has a high impact on the displacements, especially in horizontal direction. The buckling changes when the connector stiffnesses is lowered. Comparing the two first buckling modes shows that the eigenvalue decreases. It is also worth pointing out that the rest of the eigenvalues are also lower and that local buckling takes place in more positions on the roof. This can be a model issue rather than an issue that is represented in real life. Whether or not the buckling in the bottom-chord disappears is hard to say. It is probably still there; it just so happens that a lot of different points in the plate buckles before it. When the stiffness decreases in the fastener, the force distribution changes from a distribution that is split 20/60/20% over the top-chords to a 25/50/25% split which means that the CGI-plates does not resemble a continuous beam.

Stiffnesses below 10^6N/m were tried, but it was found that it is impossible to have a stiffness that is below 10^6N/m since the too low stiffness made the CGI-plates fall off since the CGI-plates didn't have the stiffness required for applied load.

Sheet thickness

The sheet thickness does impact displacement vertically and horizontally, especially horizontally. A thick CGI-plate will deform less, thus it will change the load distribution of the model. Since the thicker CGI-plate doesn't give away, it becomes stiffer and the stress of the outer top-chords increases. Since the vertical deformation decreases, the rotation of the outer top-chords decreases, thus decreases the horizontal deformation on the outer top-chords.

The non-linear analysis shows that the deformation decreases approx. 28% with a four times thicker CGI-plate.

The buckling analysis showed that the buckling load increases by 8.5 % when the thickness is changed from $0.8\ mm$ to $3.2\ mm$ which means that the thickness of the CGI-plate does not affect the eigenvalue as much as originally thought. The buckling in the CGI-plate is removed in the earlier buckling modes with a thicker sheet since the plates are more stable and not prone to buckle. The results in prentices in table 24 are not compared to each other, since it is only the eigenvalue for the bottom-chord that is interesting in this analysis.

A sheet thickness of $0.4mm$ was also tested but it was not possible for the test to reach convergence since the load was too high for that small thickness.

5.2 Overall conclusion

The study shows that it is not the top-chord that should be looked at closely, but in fact the bottom-chord. The bottom chord buckles at an eigenvalue, which was 5,5 times bigger than the applied load. So the question boils down to whether a safety factor of 5,5 is more than enough for the stability of the structure.

The analyses performed in this thesis were done without imperfections, which is something that exists in reality. Imperfections would affect the result of the simulations made. In a real-life

scenario, there would also be some type of horizontal load acting on the building which would affect the stability of the structure.

While the tested building had a bracing between the bottom-chord in one end of the building, it is not unusual that buildings of this type are built without any bracing. There would be a significant drop of the eigenvalue if this bracing was removed, while an increase of the eigenvalue would happen if a bracing was added on the other side of the building.

The studied building used a HEA 200 beam as a bottom chord and a fixed length of 25 meters. It is fair to assume that a longer length span than the one studied would result in a lower eigenvalue, since a longer span usually calls for a slenderer beam profile. A slender profile is more prone to buckle i.e. a smaller load is needed for the beam to buckle. The profile of a bottom beam can vary from a solid section, L angle, round tube, rectangular tube etc. Usually a U-profile is used for these types of trusses.

One can assume that all of these parameters would affect the eigenvalue of a structure of this type and that the values produced by this study were obtained under ideal circumstances. With this in mind, the conclusion is that even with bracing there is a risk that structures of this kind are not stable enough and the matter should be examined more so that the design of structures of this kind can be changed in the future.

The tested roof models showed that the modeling of the CGI-plates did not affect the behavior of the structure, nor did it affect the deformation. Since the results of the test of the three models where pretty much the same, my recommendation for future work is to use one of the simpler models to save time.

The results indicate that a change of CGI thickness is not a good way to increase the eigenvalue of a structure since a four times thicker CGI plate only gives an increase of 8,5 % on the eigenvalue. A thicker CGI plate will also lead to a different force distribution over the structure, which can lead to some unwanted changes in the structure. An increase of the thickness also leads to that more material is used, which increases the cost for the roof.

In conclusion, additional research needs to be done on the subject, but looking on the result of the study it is concluded that bracing absolutely is needed as extra support for structures like these.

References

Hanses, K. (2015). *Basics steel constructions .* Basel: De Gruyter.

Krenk, S. (2009). *Non-linear Modeling and Analysis of Solids and Structures.* New York: CAMBRIDGE UNIVERSITY PRESS.

Ottosen, N., & Ristinmaa, M. (2005). *The Mechanics of Constitutive Modelling.* Lund: Elsevier science.

Petersson, H., & Ottosen, N. (1992). *Indroduction to the finite element method.* Lund: University of Lund.

Pettersson, O. (1971). Knäckning. Lund: Lunds institute of technology.

Sharcnet. (n.d.). *Abaqus analysis user manual.* Retrieved 30 october, 2019, from http://dsk.ippt.pan.pl/docs/abaqus/v6.13/books/stm/default.htm?startat=undefined

Shelter cluster . (n.d.). Retrieved oktober 30, 2019, from https://www.sheltercluster.org/sites/default/files/docs/cgi_specification_150708.pdf

Timoshenko, S. P., & Gere, J. M. (1961). *Theory of elastic stability.* Singapore: McGraw Hill.

World Archaeolgy. (2008). Retrieved 12 4, 2019, from https://www.world-archaeology.com/features/history-of-corrugated-iron/

Wriggers, P. (2008). *Nonlinear Finite Element Methods.* Berlin: Springer-verlag.

Appendix A
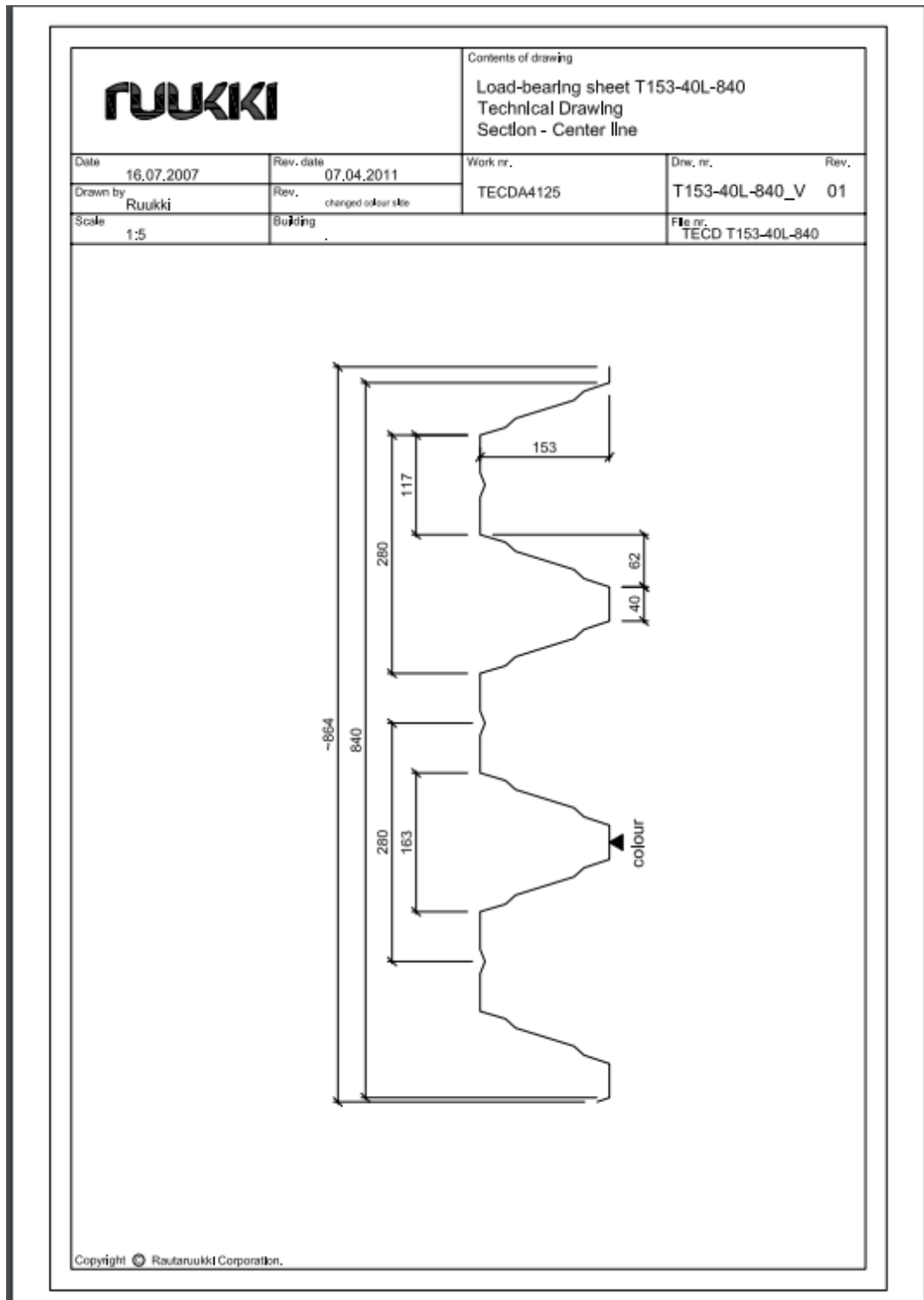
| | Contents of drawing |
| Load-bearing sheet - Insulated roof |
| Erection - General view |

ruukki		
Date 18.10.2005	Rev. date .	Work nr. IN00A4001	Drw. nr. IN 01	Rev.
Drawn by Ruukki	Rev. .			
Scale 1:25	Building		File nr. IN00A4001	

Section A - A
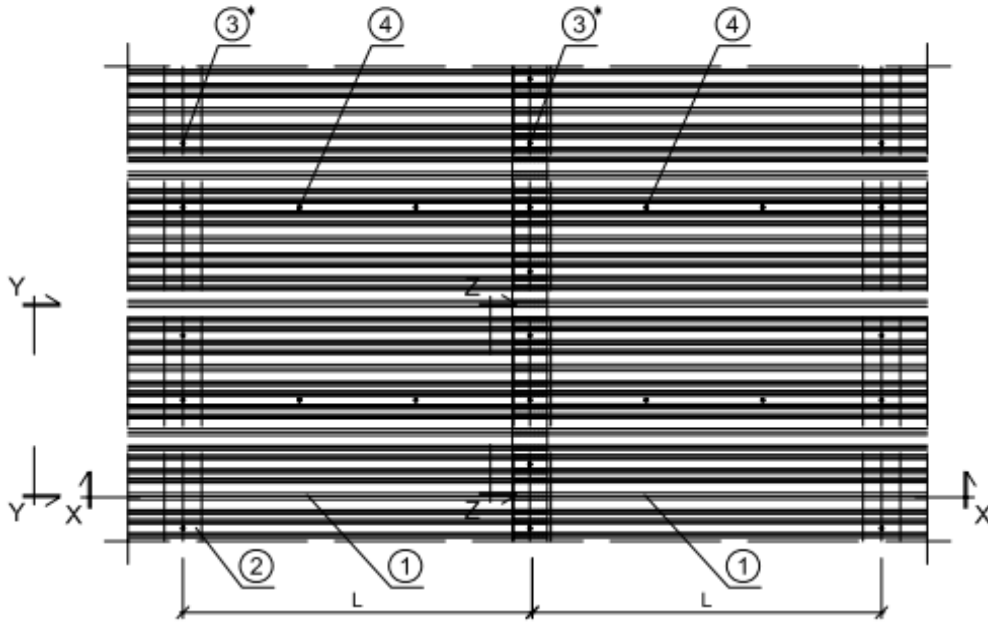
Section X - X
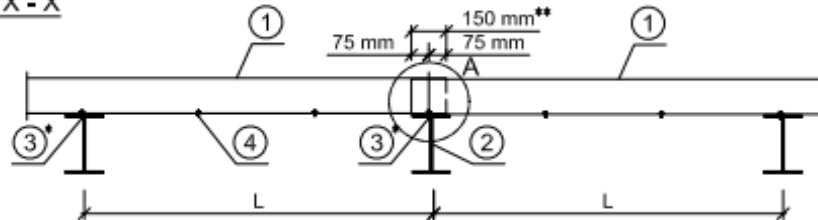
Attention:

L - span length
* - fasteners installed according to structural design
** - side overlapping according to structural design

1. Ruukki load-bearing sheet
2. Primary structure according to structural design
3. Fastener in every flange against support
4. Fastener on sidelaps c\c max 500 mm
Sections Y-Y, Z-Z drawing no IN 02, IN 03
Detail A drawing no IN 04

Contents of drawing
Load-bearing sheet - Insulated roof
Installation - Simple overlap

Date 07.04.2011	Rev. date 07.04.2011	Work nr. IN00A4007	Drw. nr. IN 07	Rev. 01
Drawn by Ruukki	Rev. .			
Scale 1:5	Building		File nr. IN00A4007	

Standard simple overlap of load-bearing sheets - Insulated roof *
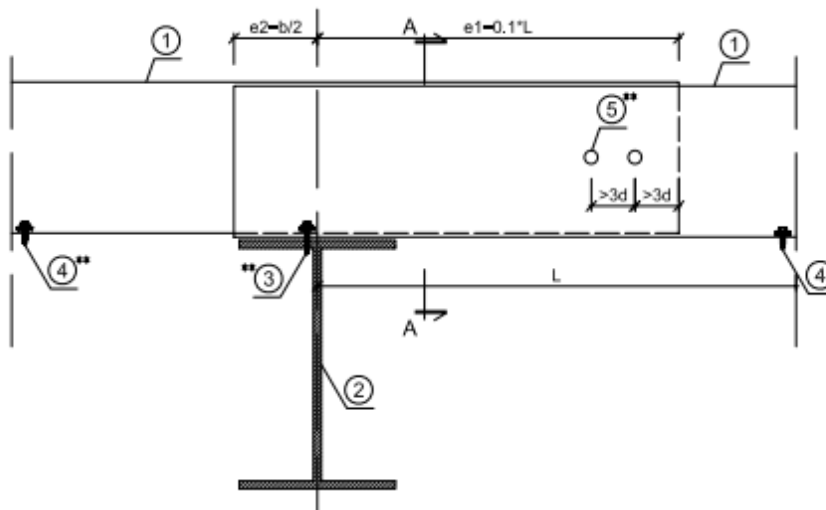
Section A - A
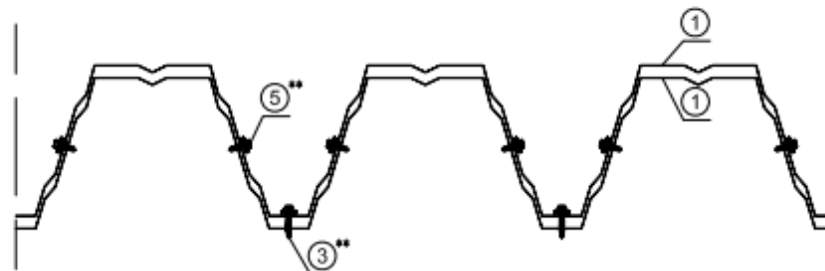
Attention:

L - span length

* - length and type of overlap according to structural design

** - number of fasteners according to structural design

1. Ruukki load-bearing sheet
2. Primary structure according to structural design
3. Fastener in every flange against support
4. Fastener on sidelaps c\c max 500 mm
5. Fastener in the web